SYNTHESIS OF ZINC OXIDE NANOPARTICLES BY SOLOCHEMICAL METHOD AND EVALUATION OF ITS ANITBACTERIAL ACTIVITY ON SELECTED DRUG RESISTANT BACTERIA

BY

MEDDA TESHOME

A THESIS SUBMITTED TO THE DEPARTMENT OF CHEMISTRY

SCHOOL OF APPLIED NATURAL SCIENCE

PRESENTED IN PARTIAL FULFILMENT OF THE REQUIRMENTS FOR

THE DEGREE OF MASTER OF SCIENCE IN CHEMISTRY

OFFICE OF GRADUATE STUDIES

ADAMA SCIENCE AND TECHNOLOGY UNIVERSITY

SEPTEMBER, 2018
ADAMA, ETHIOPIA

SYNTHESIS OF ZINC OXIDE NANOPARTICLES BY SOLOCHEMICAL METHOD AND EVALUATION OF ITS ANITBACTERIAL ACTIVITY ON SELECTED DRUG RESISTANT BACTERIA

BY: MEDDA TESHOME

ADVISOR: GEMECHU DERESSA (PhD)

CO-ADVISOR: ENYEW AMARE (PhD)

A THESIS SUBMITTED TO THE DEPARTMENT OF CHEMISTRY

SCHOOL OF APPLIED NATURAL SCIENCE

PRESENTED IN PARTIAL FULFILMENT OF THE REQUIRMENTS FOR

THE DEGREE OF MASTER OF SCIENCE IN CHEMISTRY

OFFICE OF GRADUATE STUDIES

ADAMA SCIENCE AND TECHNOLOGY UNIVERSITY

SEPTEMBER, 2018
ADAMA, ETHIOPIA

APPROVAL OF BOARD OF EXAMINERS

We, the undersigned, members of the board of examiners of the final open defense by MeddaTeshome have read and evaluated his thesis entitled "**SYNTHESIS OF ZINC OXIDE NANOPARTICLES BY SOLOCHEMICAL METHOD AND EVALUATION OF ITS ANITBACTERIAL ACTIVITY ON SELECTED DRUG RESISTANT BACTERIA**" and examined the candidate. This is, therefore, to certify that the thesis has been accepted in partial fulfillment of the requirement of the Degree of Master of Science in Chemistry.

Gemechu Deressa (PhD) Major Advisor	_____ Signature	_____ Date
Enyew Amare (PhD Co - Advisor	_____ Signature	_____ Date
_____ Chairperson	_____ Signature	_____ Date
_____ Internal Examiner	_____ Signature	_____ Date
_____ External Examiner	_____ Signature	_____ Date

DECLARATION

I hereby declare that this M.Sc Thesis is my original work and has not been presented for a degree in any other university, and all sources of material used for this thesis have been duly acknowledged.

Name: Medda Teshome

Signature:_____

This M.Sc Thesis has been submitted for examination with our approval as thesis advisors.

Advisor: Dr. Gemechu Deressa (PhD), Co-advisor: Dr. Enyew Amare (PhD)

Signature: _____ Signature: _____

Date of submission: _____ Date of submission: _____

ADVISOR'S APPROVAL SHEET

To: Chemistry Department

Subject: Thesis Submission

This is to certify that the thesis entitled "**SYNTHESIS OF ZINC OXIDE NANOPARTICLES BY SOLOCHEMICAL METHOD AND EVALUATION OF ITS ANITBACTERIAL ACTIVITY ON SELECTED DRUG RESISTANT BACTERIA"** submitted in partial fulfillment of the requirements for the degree of Master of Science in Chemistry, the Graduate program of the department of Chemistry, and has been carried out by Medda Teshome Id. No GSU/0501/06, under our supervision. Therefore, we recommend that the student has fulfilled the requirements and hence hereby he can submit the thesis to the department.

Dr. Gemechu Deressa (PhD), _____ _____

Name of Advisor Signature Date

Dr. Enyew Amare (PhD) _____ _____

Name of Co-Advisor Signature Date

DEDICATION

This thesis manuscript is dedicated to my dearly loved “son, Yusuf Medda, mother w/e Garibe Lenjiso and wife Worqie Damisie” for their concern, love, patience and affection.

ACKNOWLEDGEMENTS

First I would like to thank almighty God who gave me strength and wisdom to complete my thesis work successfully.

Here I would like to express my sincere gratitude to my advisor, Dr. Gemechu Deressa and Co-advisor, Dr. Enyew Amare for their visionary guidance, friendly approach, corrections, incredible suggestion, insightful advices and genuine supports in my master's program, without which this thesis would not have been accomplished to its least content.

I would like to extend my thanks to the department of Applied Chemistry, Adama Science and Technology University and to all our teachers, for providing us with the necessary knowledge, fruitful advice and friendly approach throughout the program and my research work.

My acknowledgement is also extended to ministry of education for letting me to join my postgraduate study and financial supporting during my study.

Last but not the least, I extend my genuine appreciation and respect to my friends for their unreserved cooperation and moral support to accomplish my study.

Finally, my cheerful thanks go to my parents and all the family members who give me moral and material support during my study.

TABLE OF CONTENTS

Contents **Page**

LIST OF FIGURES

Figures Page

LIST OF TABLES

Tables **Page**

LIST OF APPENDICES

Appendix **Page**

LIST OF ABBREVIATIONS

ATCC	American Association of Textile Chemists and Colorists
CB	Conduction band
CVD	Chemical vapour deposition
D	Average crystallite size
DMSO	Dimethyl sulfoxide
DNA	Deoxyribonucleic acid
EBSD	Electron back scatter diffraction

EDS	Energy dispersive x-ray spectrometry
FTIR	Fourier Transform Infrared
HRXRD	High resolution X-ray diffraction
K	Polarization Factor
MOCVD	Metal organic chemical vapour deposition
Nc	Negative control
NPs	Nanoparticles
Pc	Positive control
PGA	Poly(α, γ, L-glutamic acid)
PLD	Pulsed laser deposition
PVP	Polyvinylpyrrolidone
ROS	Reactive Oxygen Species
r.p.m	Revolutions per minutes.
SEM	Scanning electron microscopy
TGA	Thermal Gravimeter analysis
UV	Ultraviolet
UV-VIs	Ultraviolet visible
VB	Valence band
XRD	X – Ray Diffraction

ABSTRACT

Antibacterial activity of zinc oxide nanoparticles has received significant interest worldwide particularly by the implementation of nanotechnology to synthesize particles in the nanometer region. Therefore, the objective of this study is to synthesize and characterize zinc oxide NPs having wurtzite crystalline structure, and study its anti-bacteria activity against some selected bacteria by using solochemical method. Zinc oxide NPs were synthesized using $Zn(CH_3COO)_2.2H_2O$, $ZnCl_2.6H_2O$, $Zn(NO_3)_2.6H_2O$ and NaOH as raw materials, and distilled water and ethanol were also be used as solvents. The synthesized ZnO NPs were characterized by Thermal Gravimeter (TGA), X-ray Diffraction (XRD), Scanning Electron Microscopy (SEM), UV-Visible Spectroscopy(UV-vis) and Fourier Transform Infrared Spectroscopy (FT-IR).The XRD analysis has provided evidences that the NPs obtained by applying $Zn(NO_3)_2.6H_2O$ and $Zn(CH_3COO)_2.2H_2O$,as precursors, have pure hexagonal wurtzite crystalline structure, typical of ZnO, with average particle sizes of 21.62 nm and 35.97 nm, respectively. The variations in sizes of ZnO NPs are due to the difference in precursors, calcinations temperatures, exposure time and reaction temperature.The FT-IR analysis indicates the peaks due to vibrational phonons of ZnO NPs also confirm the successful production of ZnO NPs by this method.The UV-Vis absorbance /reflectance peak variations among the ZnO NPs are due to the difference in their size and shape, which results due to the difference in precursors and calcination temperatures. The synthesized ZnO NPs was applied and compared for antibacterial activity against Escherichia coli, Basilius subtilis, Pseudomonas aeruginosa and Staphylococcus aureus bacteria using agar well diffusion method. Among the bacterial classes tested, only the gram-positive Basilius subtilis were found to be particularly resistant to the ZnO NPs synthesized by this method. This study also revealed that the ZnO NPs synthesized from the hydrated forms of Zinc nitrate, Zinc chloride and Zinc acetate have budding antibacterial activity against Escherichia coli, Pseudomonas aeruginosa and Staphylococcus aureus bacteria because ZnO-NPs exhibit attractive antibacterial properties due to increased specific surface area as the reduced particle size leading to enhanced particle surface reactivity.

***Keywords**: Zinc oxide nanoparticles, Anti-bacterial activity, Morphology, Escherichia coli, Staphylococcus aureus, Basilius subtilis, Pseudomonas aeruginosa.*

1. INTRODUCTION

1.1 Background of the Study

Bacterial contamination continues to draw public attention. It is estimated that approximately 48 million cases of pathogenic diseases occur in the United States (Morris, 2011). Therefore, in order to solve this problem, it is highly necessary to develop effective antibacterial agents to control the bacterial population. Generally, antibacterial agents can be categorized as organic or inorganic antibacterial agents. Organic antibacterial agents such as organic acids, essential oils, bacteriocins and enzymes have been widely studied. However, they have some shortcomings, such as low resistance to processing conditions, which limit their applications. As a result, inorganic antibacterial agents have attracted much interest for bacterial control (Jung, *et al*., 2008). The main advantages of inorganic antibacterial agents, compared to organic antibacterial agents, are the improved stability under harsh processing conditions (Makhluf, *et al*., 2005). Presently, some of the inorganic antibacterial materials, in particular inorganic metal oxides such as TiO_2, ZnO, MgO and CaO, have been studied (Sawai, 2003). Among the studied inorganic metal oxides, ZnO, MgO and CaO are of particular interest because they are not only stable under harsh process conditions, but also generally regarded as safe materials to human beings (Sundrarajan, *et al.,* 2012). Additionally, they have antibacterial activity without photo-activation, compared to TiO_2 that requires photo-activation in nanoscience (Manna, 2012).

Nanotechnology is basically an amalgamation of two words “Nano” and “Technology” that deals with dimensions and tolerances of less than 100 nanometers, especially the engineering of individual atoms and molecules. Nanoparticles are a special group of materials with unique features and extensive applications in diagnostic techniques, drug delivery, sunscreens, antimicrobial bandages, disinfectant, a friendly manufacturing process that reduce waste products, as catalyst for greater efficiency in current manufacturing process by minimizing or eliminating the use of toxic materials, to reduce pollution and an alternative energy production (Sobha, 2010). In this regard, nanoparticles are recognized as antibacterial agents due to their size, structure, and surface properties (Raghupati, *et al*., 2011). Among the metal oxide nanoparticles, Zinc oxide has high chemical stability, strong photosensitivity and non-toxicity

property and is widely used in antibacterial materials (Zanni, *et al*., 2011). It is usually insoluble in water and appears as a white powder. The powder is widely used as an additive into numerous materials and products including plastics, ceramics, glass, cement, rubber, lubricants, paints, ointments, adhesives, sealants, pigments, foods (source of Zn nutrient), batteries, fire retardants, etc. Compared with ordinary ZnO powder, ZnO nanoparticles have a large specific surface area and small size effect, and show wide application potential in microbial inhibition and mildew removal (Li, *et al.,* 2012; Cha, *et al*., 2015).

In this study, the different sizes, shape and morphology of ZnO NPs were synthesized using $Zn(NO_3)_2.6H_2O$, $ZnCl_2.6H_2O$ and $Zn(CH_3COO)_2.2H_2O$ as precursors, at 70^oC and 90^oC reaction temperature through solochemical method for the inhibition of *Staphylococcus aureus*, *Basilius subtilis*, *Pseudomonas aeruginosa* and *Escherichia coli* bacteria. These four bacterial strains were selected as they are highly contagious; hence one can evaluate and compare the potential antibacterial activity of zinc oxide nanoparticles. The product obtained was characterized by X-ray diffraction (XRD), Thermal gravimeter (TGA), Fourier transform infrared spectroscopy (FT-IR), Scanning electron microscopy (SEM) and Energy dispersive X-ray spectroscopy (EDX) modern techniques.

1.2 Statement of the Problem

Bacterial infectious diseases are serious health problem that has drawn the public attention in worldwide as a human health threat, which extends to economic and social complications. In recent years, the number of infections associated with antibiotic-resistant bacteria has steadily increased.The need for novel antibiotics comes from the relatively high incidence of bacterial infection and the growing resistance of bacteria to conventional or traditional antibiotics such as penicillin and gentamyicin. Consequently, new methods for reducing bacteria activity (and associated infections) are badly needed. Nanotechnology, the use of materials with dimensions on the atomic or molecular scale, has become increasingly applied to medical applications and is of great interest as an approach to killing or reducing the activity of numerous microorganisms. This shows that, nanoparticles, which rely on entirely different mechanisms of antibacterial

activity than traditional antibiotics, are an intriguing alternative. ZnO NP is currently being considered as an antibacterial agent in both micro as well as nano scale formulations.

This study may provide important information about the implementation of nanoscience, or the use of materials with nanoscale dimensions in studying and synthesizing the ZnO nanoparticles from most common cheap precursors and compare the antibacterial properties of the synthesized ZnO NPs on bacteria. It may also indicate how the different parameters such as types of precursors, chemical reaction temperature, reaction time, etc. employed in the synthesis of nanomaterials; influence the crystal size and structure of ZnO nanoparticles synthesized.

1.3 Objectives of the Study

1.3.1 General objective

The general objective of this study is to synthesize and characterize zinc oxide nanoparticles using the solochemical method, and evaluate their antibacterial activity on four selected bacterial strains.

1.3.2 Specific objectives

The specific objectives of this study are to:-

- Synthesis ZnO nanoparticles from Zinc acetate dihydrate, Zinc chloride hexahydrate and Zinc nitrate hexahydrate precursors using solochemical method.
- Characterize the synthesized ZnO nanoparticles by using modern techniques such as SEM, FT- IR, XRD, EDX,UV-vis and TGA.
- Investigate the effect of the different parameters such as temperature, type of precursor, and calcination time on crystal size of ZnO nanoparticles synthesized.
- Evaluate antibacterial activity of the synthesized ZnO NPs from three precursors under different parameters against *Staphylococcus aureus*, *Basilius subtilis*, *Pseudomonas aeruginosa* and *Escherichia coli* bacteria.
- Compare the crystalline size and antibacterial activity of ZnO NPs synthesized from the three precursors.

1.4 Significance of the Study

This study will provide important information about the solochemical synthesis of ZnO nanoparticles from three different starting materials and its biological application. It may also provide important information about how the different parameters such as precursors, temperatures and calcination times affect the size and activity of ZnO NPs. Furthermore, it can provide important information for the researchers who are interested to conduct further studies especially on the synthesis of ZnO NPs from zinc chloride hexahydrate.

1.5 Scope of the Study

This synthesis technique is limited to solochemical method of ZnO nanoparticles preparation, and their characterization might also be limited to TGA, XRD, SEM, EDX, UV-vis and FT-IR modern techniques. In addition to these, their antibacterial application against drug resistant bacteria might also be limited to only the uncalcinated sample of ZnO NPs synthesized from zinc nitrate hexahydrate and the calcinated samples of ZnO NPs synthesized from three different precursors.

2. LITERATURE REVIEW

2.1 Methods for the Synthesis of Nanoparticles

Selection of the synthesis method to realize required NPs largely depends on the desired size, appropriate surface properties and the type of concerned material such as metals, semiconductors, ceramics, and polymers. These methods determine the physicochemical characteristics of the metal oxide nanoparticles, such as the size, disparity, type of intrinsic and/or extrinsic defects, morphology and crystal structure. High-throughput NPs with good and controlled quality are desirable for their commercialization in various fields of applications. There are two basic approaches commonly employed to prepare nanoparticles, namely:

(1) Top-down approach, where synthesis is initialized with the bulk counterpart that leaches out systematically bit-after-bit leading to the generation of fine nanoparticles. Photolithography, electron beam lithography, milling techniques, anodization, ion and plasma etching are some of the commonly used top-down methods for the mass production of NPs.

(2) Bottom-up approach - involves the coalescence or assembling of atoms and molecules to generate diverse range of nanoparticles. Examples of bottom-up approach include self-assembly of monomer / polymer molecules, chemical or electrochemical nonstructural precipitation, sol–gel processing, laser pyrolysis, chemical vapour deposition (CVD), plasma or flame spraying synthesis and bio-assisted synthesis. Based on the type of the medium in which the oxidation reaction takes place, nanoparticles synthesis methods can be divided in three categories, namely- solution based (sonochemical), vapor state and biological methods. In general, nanoparticles synthesis methods can also be divided in three groups: physical, chemical and bio-assisted methods (Daraio, *et al*.,2012).

2.1.1 Physical methods for the synthesis of nanoparticles

Physical methods apply mechanical pressure, high energy radiations, thermal energy or electrical energy to cause material abrasion, melting, evaporation or condensation to generate NPs. These methods mainly operate on top-down strategy and are advantageous as they are free of solvent

contamination and produce uniform monodisperse NPs. At the same time, the abundant waste produced during the synthesis makes physical processes less economical. High energy ball milling, laser ablation, electro spraying, inert gas condensation, physical vapour deposition, laser pyrolysis, flash spray pyrolysis, melt mixing are some of the most commonly used physical methods to generate nanoparticles.

2.1.2 Chemical methods for the synthesis of nanoparticles

Solochemical, precipitation and co-precipitation, microemulsion, Sol–gel, hydrothermal synthesis, polyol synthesis, chemical vapor synthesis and plasma enhanced chemical vapor deposition techniques are some of the most commonly used chemical methods for the nanoparticles synthesis.

2.1.2.1 Solochemical method of ZnO nanoparticles synthesis

Among the routes for chemical synthesis of ZnO nanoparticles in industrial scale, the solochemical method stands out due to its rapidity, versatility, simplicity, low cost and it provides a high uniformity of the final product (Hu and Chen,2008). Besides these, it has the ability to produce ZnO nanoparticles with different particles size and morphology by using different precursors and calcination temperature. This technique consists basically in the reaction between a heated alkaline solution and a zinc containing complex under controlled temperature. As a method for preparing high-quality ZnO powders, the solochemical synthetic method has advantage to obtain high crystallized powders and with high purity in short reaction times and in relatively low temperatures, without necessity of any posterior treatments. The particle properties such as morphology and size can be altered via this method by adjusting of parameters such as reaction temperature, calcination temperature, concentration and reaction time.

2.1.2.2 Precipitation and thermal decomposition methods of nanoparticles synthesis

Among the various methods of nanoparticles synthesis, precipitation is one of the most important methods to prepare nanoparticles; the method reduces the temperature of the reaction where homogenous mixtures of the reagents precipitate. It is simple method for the synthesis of nano-

powders of metal oxides, which are highly reactive in low temperature sintering. It involves precipitating the oxo-hydroxide form from a solution of a salt precursor (metal salts like nitrates or chlorides) in a solvent (like water) by using a precipitating medium. Once a critical concentration of species in solution is reached, a short burst of nucleation occurs followed by growth phase. In a typical chemical precipitation method, a reducing agent (mostly inorganic alkaline) is allowed to react with the precursor and the fractional precipitation of a specified ion in a solution results in the precipitation not only of the target ion but also of other ions existing in the solution. A resultant soluble or insoluble precipitate produced in the technique is washed, dried and calcined at different temperatures to obtain the particular nanoparticles with desired morphology and characteristics.

Some reaction mechanisms involved in the preparation of ZnO nanoparticles from zinc nitrate and sodium hydroxide precursors by the precipitation method are:

$$2NaOH_{(s)} \longrightarrow 2Na^{+}_{(aq)} + 2OH^{-}_{(aq)} \quad \text{..... (1)}$$

$$Zn(NO_3)_2.6H_2O_{(s)} \longrightarrow Zn^{2+}_{(aq)} + 2NO^{-}_{3\,(aq)} + 6H_2O_{(aq)} \quad \text{..... (2)}$$

$$Zn^{2+}_{(aq)} + 2OH^{-}_{(aq)} + x\,H_2O_{(aq)} \longrightarrow Zn(OH)_2.X\,H_2O_{(s)}\downarrow \quad \text{..... (3)}$$

$$Zn(OH)_2.X\,H_2O_{(s)}\downarrow \longrightarrow Zn(OH)_{2\,(s)} + X\,H_2O_{(g)} \quad \text{.....(4)}$$

$$Zn(OH)_{2\,(s)} \longrightarrow ZnO_{(s)} + H_2O_{(g)}\uparrow \quad \text{..... (5)}$$

2.1.2.3 Sol–gel precipitation method for nanoparticles synthesis

The sol-gel technique is one of the fastest growing fields of contemporary chemistry (Abd El-Latif *et al*., 2011). It is the two stage solochemical process that produces nanometric powders used initially to produce ZnO, where an initial solution containing a zinc complex is decomposed to form nanometric powder zinc oxide. Hydrolysis and condensation are the typical steps of sol–gel process, in which the former uses water to disintegrate the bonds of the precursor that is also the first step in formation of the gel phase. This process is then followed by condensation that

leads to the formation of nanomaterials after which excess water is removed to determine the final structure of the material. Generally, sol-gel processing is a wet chemical synthesis approach that can be used to generate nanoparticles by gelation, precipitation, and hydrothermal treatment (Rao, *et al.,* 2004). For sol–gel growth generally, the required sol (colloidal suspension of solid particles in the liquid) is prepared and the template is put into the sol for a required period (example. 0.5–1 hour). After removing the membrane from the sol it is dried and then annealed at higher temperature before the required phase is formed. The mixture is then heated on a hot plate till a sol of desired viscosity is formed.

2.1.2.4 Polyol process of nanoparticles synthesis

Polyol process is the synthesis of metal-containing compounds using poly (ethylene glycol) as the reaction medium, which plays a role of solvent, reducing agent and complexing agent at the same time, with dissolved stabilizing / protecting agents (Rahman, 2009). This chemical process is used to synthesize a wide range of metal based nanoparticles (Ag, Pt, Pd, Pr, and Cu), metal oxide nanoparticles (ZnO, Gd_2O_3, and Cu_2O), magnetic NPs and metal hybrid NPs.

2.1.2.5 Synthesize of ZnO nanoparticles in alkaline solution

ZnO nanostructures can be synthesized through various methods such as sputtering technique, vapour deposition, polyol synthesis, pulsed laser deposition (PLD), metal organic chemical vapour deposition (MOCVD), thermal decomposition, and sol-gel methods, by controlling the synthesis parameters. The properties can be tailored by shape and size, resulting in renewable applications relevant to their structural properties. Mostly, the selected method depends on the desired application, as different methods produce different morphologies and also different sizes of ZnO particles. Accordingly, the chemical and physical parameters such as the solvent type, precursors, pH, and the temperature are highly considered during the synthesis of ZnO nanoparticles.

An alkaline solution is essential for the formation of ZnO nanostructures because normally divalent metal ions do not hydrolyze in acidic environments (Demianets, *et al*., 2002). The commonly used alkali compounds are potassium hydroxide (KOH) and sodium hydroxide

(NaOH). In general, the solubility of ZnO in an alkali solution increases with the alkali concentration and temperature. Super saturation allows a growth zone to be attained. KOH is thought to be preferable to NaOH, because K^+ has a larger ionic radius and thus a lower probability of incorporation into the ZnO lattice. Furthermore, it has been suggested that Na^+ is attracted by the OH^- around the nanocrystal and forms a virtual capping layer, thus, inhibiting the nanocrystal growth **(**Viswanatha, *et al*., 2007). The main reactions involved in the growth are given in Equations 6 to 10 (Demianets, *et al*., 2002). For the Equation (7), the product is not necessarily $Zn(OH)_4^{2-}$, but could also be $Zn(OH)^+$, $Zn(OH)_2$, or $Zn(OH)_3^-$, depending on the parameters, such as the concentration of Zn^{2+} and the pH value.

$$Zn^{2+} + 2OH^- \rightleftharpoons Zn(OH)_2 \quad \text{..... (6)}$$

$$Zn(OH)_2 + 2OH^- \rightleftharpoons [Zn(OH)_4]^{2-} \quad \text{..... (7)}$$

$$[Zn(OH)_4]^{2-} \rightleftharpoons ZnO_2^{2-} + 2H_2O \quad \text{..... (8)}$$

$$ZnO_2^{2-} + H_2O \rightleftharpoons ZnO + 2OH^- \quad \text{..... (9)}$$

$$ZnO + OH^- \rightleftharpoons ZnOOH^- \quad \text{..... (10)}$$

At the very beginning of the growth process, Zn^{2+} and OH^- ions coordinate with each other, and then they undergo dehydration by proton transfer, forming Zn^{2+}--- O^{2-} --- Zn^{2+} bonds and leading to agglomerate. These aggregates usually contain fewer than 50 ions, and the formation of O^{2-} ions implies dramatic changes within the aggregate. After the aggregates reach around 150 ions, wurtzite type (tetrahedral coordination) ZnO domains are then nucleated in the central region of the aggregates (Zhang, *et al*., 2002). Aggregates of over 200 ions exhibit a nanometer sized core of the wurtzite structured ZnO which grows as a result of further association and dehydration of Zn^{2+} and OH^- ions. In equations 6 to10, the O^{2-} in ZnO comes from the base, not from the solvent H_2O. Therefore growth of ZnO does not necessarily require the solvent to be H_2O (Zhang*, et al*., 2002). It could be organic solvents, such as methanol, ethanol, butanol, etc. Under alkali conditions, the reactions could take place at room temperature by adjusting the ratio of Zn^{2+} and OH^-, giving rise to ZnO nanowires with diameter even below 10 nm. ZnO nanowires with various aspect ratios can be prepared by simply adjusting OH^- concentration and reaction time

(Cao, *et al.,* 2006). The advantages associated with sonochemical methods include uniform size distribution, a higher surface area, faster reaction time and improved phase purity of the metal oxide nanoparticles.

2.1.3 Bio-assisted methods for the synthesis of nanoparticles

Green synthesis provides an environmentally benign, low-toxic, cost-effective and efficient protocol to synthesize and fabricate nanoparticles. Biosynthesis of nanoparticles is a kind of bottom up approach where the main reaction occurring is reduction/oxidation. The microbial enzymes or the plant phytochemicals with anti-oxidant or reducing properties are usually responsible for reduction of metal compounds into their respective nanoparticles. These methods employ biological systems like bacteria, fungi, viruses, yeast, plant extracts, etc. for the synthesis of metal and metal oxide nanoparticles. Bio-assisted methods can be broadly divided into three categories:

2.1.3.1 Biogenic synthesis using microorganisms

Prokaryotic bacteria, actinomycetes, fungi, algae and yeast are extensively used as bio-reactors for the synthesis of nanoparticles. This synthesis can be classified into intracellular and extracellular depending upon the location of nanoparticles synthesis. The intracellular method involves transporting of metal ions into the microbial cell to form nanoparticles in the presence of enzymes. The extracellular synthesis of nanoparticles involves trapping of metal ions on the surface of the cells and reducing ions in the presence of enzymes (Zhang, *et al*., 2011).

2.1.3.2 Plant extracts for nanoparticles synthesis

Biosynthesis of nanoparticles using plant extracts or plant biomass is one of the very effective, rapid, clean, non-toxic and eco-friendly methods. This method has been utilized predominantly to synthesize nanoparticles of noble metals, metal oxides, and bi-metallic alloys.

2.1.3.3 Bio molecules as templates to design nanoparticles

Various bio molecules like nucleic acids, membranes, viruses and diatoms are used as templates to synthesize nanoparticles. DNA is widely known as an excellent bimolecular template that has a strong attraction with transition metal ions.

2.2 Environmental Implications on Synthesis of ZnO NPs

The nature of biological entities and its concentrations in combination with organic reducing agents influence the size and shape of nanoparticles (Aromal, *et al*., 2012).Moreover, size and shape of nanoparticles strongly depend on the growth medium parameters such as pH,solvent percentage, reflux temperature, calcination temperature, exposure timeand concentration of precursors (Gericke, *et al*., 2006). Bio-reduction of metal precursors takes place either in **vitro** or in **vivo** for the synthesis of nanomaterials. However, enzymes, proteins, sugars, and phytochemicals, like flavonoids, phenolics, terpenoids, cofactors etc., mainly act as reducing and stabilizing agents (Kaushik, *et al*., 2010).

2.2.1 Capping agents and stabilizers

Usually, antibacterial tests are done in aqueous media or cell culture media. ZnO is known as nearly insoluble in water, it agglomerates immediately with water during synthesis due to the high polarity of water leading to deposition. Issues of aggregation, re-precipitation, settling, or non-dissolution impede the synthesis processes. In this regards, a number of researchers considered this difficulty by using certain additives that have no significant effect in the antibacterial activity.The addition of polymers such as polyvinylpyrrolidone (PVP), polyethylene glycol (PEG) and poly (α, γ, L-glutamic acid) (PGA) as stabilizers enhanced ZnO morphology and size for the antibacterial activity. In chemical synthesis, capping agents (citric acid, extracellular proteins, enzymes, alcohols, ketons, aldehydes, amines, carboxylic acids, etc) and stabilizers are extensively used in order to control the size and to avoid agglomeration. After addition of those chemicals, the mixtures are exposed to vigorous vortex (e.g., 5 min) or kept overnight on magnetic stirring and then ultrasonicated 20–30 min to avoid aggregation and deposition of particles. Characterization of ZnO-NPs is required to identify factors impacted

stability such as particle size, pH of solution, structural, morphological, and surface properties, these factors in turn have effect on the bioactivity.

2.2.2 Reducing agents and pH

Most of the synthetic techniques for ZnO utilize a reducing agent to reduce a respective zinc salt and vigorous synthetic environment that involves either highly acidic or basic conditions. Precipitation/co-precipitation method mainly employs sodium hydroxide (NaOH) as reducing agent, which is highly corrosive and degrades all kinds of protein. Dissolution of NaOH in water is exothermic and may cause heat burns or may ignite. In the synthesis of ZnO, excessive amounts of NaOH with higher molar concentrations and pH are used to ensure the reaction completion.

2.2.3 Temperature

The deposition time of nano-ZnO in aqueous solution presents a trend of first increases then decrease. This is due to the temperature has an impact on super-saturation of solution, which relates with the nucleation rate in system. As the temperature rises, the faster reaction rate and the increasing of super-saturation of reaction products lead to crystal core forming rate is accelerated in the short reaction time, that means the controlling step of the reaction is transferred from grain growth to crystal nucleus formation, so the particles are smaller. With the temperatures continuing to rise, the phenomenon of "nuclear-aggregation" caused by the rapid formation of crystal nucleus is obvious that result in forming aggregate among the crystal nucleus. The major disadvantage of the high temperature processes is the consumption of the energy. Majorly, heat evolving from high temperature processes may cause heat edema, heat rashes, heat cramps, heat exhaustion, heat syncope, and heat strokes (Koser, 2011). A number of methods in synthesis of ZnO NP involve high temperatures, for example, hybrid electrochemical thermal method (60–700^{0}C) (WenJ.et al., 2014), high temperature mixing hydrothermal processes (160–200^{0}C), etc.Because the particle size and annealing temperature have a close relation, with increases of annealing temperature, particle size increases (Vidyasagar, *et al*., 2012). Annealing process may be responsible for the occurrence of dislocation and

adsorption/decomposition on the surface, thus the structure and stoichiometric ratio of the material would change. Studies indicate thatgenerally elevation of increasing calcination temperature produces increase in particle size due to aggregation and also unevenly sized particles. Thus, crystallite size of ZnO nanoparticles increases gradually by the elevation of calcination temperature in ionic liquid compared to conventional solvent as medium.

2.3 Properties of ZnO Nanoparticles

Zinc oxide is a chemical compound found naturally in the mineral called zincite and has attracted much attention in recent times due to its low cost and because it can be obtained by simple techniques(Koudelka, *et al*., 2014). Most of the group II-VI binary compound semiconductors crystallize in either cubic zinc-blende or hexagonal wurtzite structure where each anion is surrounded by four cations at the corners of a tetrahedron, and vice versa. This tetrahedral coordination is typical of sp^3 covalent bonding, but these materials also have a substantial ionic character. ZnO is II-VI compound semiconductor whose ionicity resides at the borderline between covalent and ionic semiconductor. The crystal structures shared by ZnO exhibits three crystallize structures namely, wurtzite, zinc-blende and an occasionally noticed rock-salt, as schematically shown in Figure1. ZnO crystallizes in the typical wurtzite hexagonal structure where oxygen and zinc atoms are spatially arranged in a way that O atoms are arranged in a closed hexagonal structure, while the Zn atoms occupy the centre of the distorted tetrahedron structure. The lattice parameters of a semiconductor usually depend on the factors:- (I) Free electron concentration acting via deformation potential of a conduction-band minimum occupied by these electrons, (ii) Concentration of foreign atoms and defects and their difference of ionic radii with respect to the substituted matrix ion, (iii) External strains for example, those induced by substrate, and (iv) Temperature.

The lattice parameters of any crystalline material are commonly and most accurately measured by high resolution x-ray diffraction (HRXRD) using the Bond method for a set of symmetrical and asymmetrical reflection. For the wurtzite ZnO, lattice constants at room temperature determined by various experimental measurements and theoretical calculations are in good agreement. The lattice constants mostly range from 3.2475 to 3.2501 Å for the “a” parameter and

5.2042 to 5.2075 Å for the "c" parameter. The c/a ratio varies in a slightly wider range from 1.593 to 1.6035. The deviation from the ideal wurtzite crystal is probably due to lattice stability and ionicity.

ZnO is a semiconductor material of the II-VI group with a large energy gap around Eg = 3.37 eV, a large range of excitation energy and controlled electrical conductivity (Look *et al*., 2002), and when doped with transition metals, it exhibits the ferromagnetic phenomenon at room temperature, and because of that it has attracted much interest due to their potential applications in "spintronics" (Prellier, *et al.,* 2003). Due to a relatively large direct band gap (~3.37 eV) of ZnO at room temperature, pure ZnO is colorless and transparent. The advantages associated with a large band gap include higher break down voltages, ability to sustain large electric fields, lower electronic noise, and high-temperature and high-power operation. Nanocrystalline powders, due to their average particle size (below 100 nm), may show different behaviors resulting from a higher surface energy due to the large surface area and the wider gap between the valence band and conduction band, effects characteristic of sizes close to the atoms. These phenomena may increase the potential use of the material, including optical, chemical, and electromagnetic, among other properties. Generally, zinc oxide NPs has unique physical and chemical properties, such as high chemical stability, high electrochemical coupling coefficient, broad range of radiation absorption and high photo stability. Therefore, because of its exceptional physical and chemical characteristics (Kwon, *et al.,* 2002), the nano-size zinc oxide is an important raw material for many applications as the design of varistors, gas sensors, luminescent oxides, rubber, paints, ceramics, and others (Perez-Lopes, *et al*., 2005).

The ZnO is insoluble in water and ethanol but is soluble in dilute mineral acids and is a fine powder, white or slightly yellow. In large quantities and high purity, it is recommended for use in the pharmaceutical, food and cosmetic industries. Zinc is a transition metal and semi-metal that can react with both acids and bases providing water and salt. Because ZnO presents intermediate properties between acid and basic oxides, it can behave as both acid and basic oxide.

It is an intrinsic n-type semiconductor material that crystallizes in the hexagonal crystal system; it is relatively inexpensive, presents low toxicity, and is very effective in protecting against UV rays. The intrinsic properties of NPs such as ZnO, TiO_2, and Ag are mostly characterized by their size, composition, crystallinity, and morphology. Reducing the size to nanoscale can modify their chemical, mechanical, electrical, structural, morphological, and optical properties. These modified features allow the NPs to interact in a unique manner with cell biomolecules and thus facilitate the physical transfer of NPs into the inner cellular structures.ZnO is a wide band gap semiconductor that displays luminescent properties in the near ultra violet and the visible regions. The emission properties of ZnO nanoparticles in the visible region widely depend on their synthetic method as they are attributable to surface defects. ZnO is an excellent material for the manufacture of sunscreen, because it absorbs ultraviolet (UV) rays and combat the potential problems associated with sun exposure. In general, when ZnO is reduced to nanoscale, it shows unique properties in comparison to its bulk counterpart. These unique properties of ZnO NPs are due to enhanced surface area, which allows for increased interaction of nanoparticles with bacteria (Jones, *et al.,* 2008). This permits using a smaller amount of Zinc Oxide NPs for the same or improved biostatic behavior.

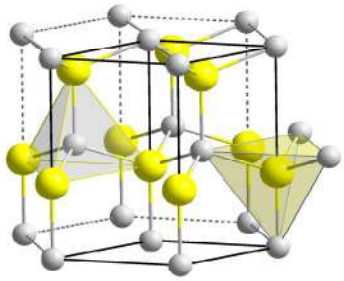

(a)Hexagonal wurtzite structure

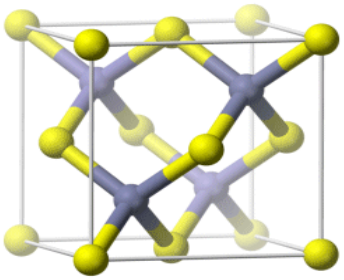

(b) Zinc blende structure

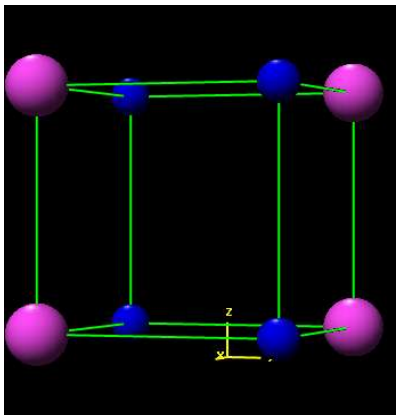

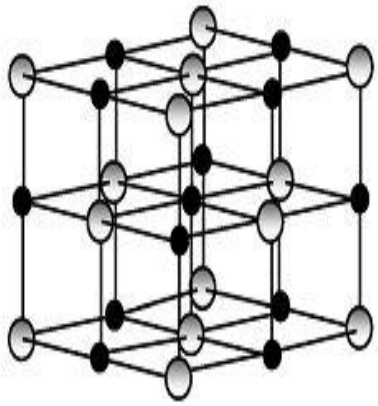

(c) Rock salt structure

Figure 1 : Crystal structures of Zinc Oxide.

2.4. Industrial Applications of Zinc Oxide and ZnO Nanoparticles

Zinc Oxide (ZnO) is analyzed to be a technologically remarkable material having a broad field of applications like semiconductor, gas sensor, piezoelectric sensor, electro luminescent material, magnetic material and actuator, ingredients of cosmetics (Meisam, *et al*., 2016). Due to the magnificent properties such as high thermal conductivity, high refractive index, binding energy, UV protection and antibacterial capabilities of Zinc Oxide, it is widely applied in various products and materials, including medicine, cosmetics, solar cells, foods, rubber and concrete. ZnO is basically included in some cosmetic lotions as it is also known to maintain UV

blockingand absorbing capabilities. ZnO can also be used as the astringent for wounds healing, anti-hemorrhoids, eczema and excoriation in the human medicine (Ozgu*et al*., 2010).

ZnO nanoparticles have recently fascinated consideration owing to its unique features. There are potentially numerous promising applications of ZnO nanoparticles in veterinary sciences due to their wound healing, antibacterial, antineoplastic and antigenic properties.Most activities to conflict and have centered on the nanocoatings or nanocomposites using nanoparticles of silver and zinc oxide. Zinc oxide nanoparticles are nontoxic that shows good evidence of antibacterial activity with increases in decreasing the particle size. Therefore, antibacterial activity of ZnO nanoparticles is remarkable application in designing microbial resistant articles for preserving food and wood products, cosmetics, novel nanomedicines wound dressing and disinfecting agents.

Hence, this study makes use of this property to inhibit growth of *Escherichia coli*, *Basilius subtilis*, *Pseudomonas aeruginosa* and *Staphylococcus aureus* bacteria using agar well diffusion method. These four bacterial strains were selected as they are highly contagious; thus, one can evaluate the potential antimicrobial activity of zinc oxide nanoparticles.

2.5 Antibacterial Activity of ZnO Nanoparticles

Bacteria are generally characterized by a cell membrane, cell wall, and cytoplasm. The cell wall lies outside the cell membrane and is composed mostly of a homogeneouspeptidoglycan layer (which consists of amino acids and sugars). The cell wall maintains the osmotic pressure of the cytoplasm as well the characteristic cell shape. Gram-positive bacteria have one cytoplasmic membrane with multilayer of peptidoglycan polymer and a thicker cell wall (20–80 nm). Whereas gram-negative bacteria wall is composed of two cell membranes, an outer membrane and a plasma membrane with a thin layer of peptidoglycan (Fu, *et al*., 2008) with a thickness of 7–8 nm. Nanoparticles size within such ranges can readily pass through the peptidoglycan and hence are highly susceptible to damage. The cytoplasm, a jelly-like fluid that fills a cell, involves all the cellular components except the nucleus. The functions of this organelle include growth, metabolism, and replication. Consequently, the cytoplasm contains proteins, carbohydrates,

nucleic acids, salts, ions, and water (~80 %). This composition contributes in the electrical conductivity of the cellular structure. The overall charge of bacterial cell walls is negative.

Antibacterial activity is known according to the American Heritage Medical Dictionary 2007, as the action by which bacterial growth is destroyed or inhibited. It is also described as a function of the surface area in contact with the microorganisms (Wahab*et al*., 2010). Antibacterial agents are selective concentration drugs capable to damage or inhibit bacterial growth and they are not harmful to the host. An antibacterial agent is considered as bactericidal if it kills bacteria or as bacteriostatic if it inhibits their growth. ZnO NP is currently being considered as an antibacterial agent in both micro as well as nano scale formulations. ZnO nanoparticles exhibit attractive antibacterial properties due to increased specific surface area as the reduced particle size leading to enhanced particle surface reactivity. The enhanced antibacterial activity of ZnO NPs can be attributed to impact of UV illumination, ZnO particle properties (size, concentration, morphology, and defects), particle surface modification, and minimum inhibitory concentration, which are represented by Figure 2.

2.5.1 UV illumination effect

ZnO is found to possess high photo catalytic efficiency among all inorganic photo catalytic materials, and is more biocompatible than TiO_2 (Fu G. et al., 2008) because it can highly absorb UV light, thus its conductivity dramatically enhances, and this feature significantly activates the interaction of ZnO with bacteria. ZnO nanoparticles in aqueous solution under UV radiation have phototoxic effect that can generate reactive oxygen species (ROS) such as hydrogen peroxide (H_2O_2) and superoxide ions (O_2^-). The generated active species by UV light are capable to penetrate into the cells, thus inhibit or kill microorganisms. This process inspired the use of the photo catalytic activity of ZnO nanoparticles in bio-nanotechnology and in bio-nanomedicine for many antibacterial applications

2.5.2 Impact of ZnO morphology

ZnO morphology is determined by the synthesis conditions. Thus, desired synthesized ZnO NPs structures for best antibacterial response could be attained by controlling parameters such as

solvents, precursor types, and physicochemical settings such as temperature and pH as well as shape-directing agents. Also, under controlled growth conditions, the surface morphology is determined by the surface activity. The shape-dependent activity is explained in terms of the percent of active facets in the nanoparticles. Synthesis and growth techniques lead to holding numerous active facets in NP. Rod-structures of ZnO have (111) and (100) facets, whereas spherical nanostructures mainly have (100) facets. High-atom-density facets with (111) facets exhibit higher antibacterial activity. Currently, it has been found that greater antibacterial results could be achieved from ZnO morphologies of highly exposed (0 0 1)-Zn terminated polar facets (Tong, *et al*., 2013).

2.5.3 Influence of ZnO particle size and concentration

Particle size and concentration of ZnO nanoparticles play important roles in the antibacterial activity. The antibacterial activity of ZnO NPs directly correlates with their concentrations as reported by several studies, likewise, the activity is size dependent, however, this dependency is also influenced by concentration of nanoparticles . Larger surface area and higher concentration are accountable for ZnO nanoparticles antibacterial activity (Peng, *et al*., 2011). ZnO NPs of smaller sizes can easily penetrate into bacterial membranes due to their large interfacial area, thus enhancing their antibacterial efficiency.

2.5.4 ZnO surface defects

Other factors that play vital roles on the mechanism are surface defects and surface charges as the surfaces of ZnO NPs containing numerous edges and corners, and thus have potential reactive surface sites. In spite of its simple chemical formula, ZnO has very rich defect chemistry, which is associated with its antimicrobial activity. Surface defects strongly affect the toxicity of ZnO. The antibacterial action of ZnO NPs is due to the membrane injury caused by defects such as edges and corners, which results from the abrasive surface of ZnO.

2.6Proposed Mechanism of Antibacterial Activity of ZnO NPs

2.6.1 Reactive oxygen species (ROS) generation as the major cause of nanotoxicity

Nanoparticles cause toxicity because :-(a) Nanostructures have electronic, optical and magnetic properties that tell about the physical dimensions and breakage in the nanostructures which can lead to a unique toxic effect that is unpredictable. (b) The surfaces of nanostructures are involved in much catalytic and oxidative reaction. These reactions may induce cytotoxicity. Cytoxicity can be greater in the nanomaterial than a bulk material because surface area to volume ratio for nanoparticle is more. (c) Some nanostructures contain metals or compound with toxicity when breakdown can reduce toxic responses to the components themselves. The toxicity of ROS to bacteria is attributed to their high reactivity and oxidizing property. The toxicity of reactive Oxygen species (superoxide anion (O_2^-), hydrogen peroxide (H_2O_2), and hydroxide (OH^-)) involves the destruction of cellular components such as lipids, DNA, and proteins, as a result of their internalization into the bacteria cell membrane. The researchers explained the production of reactive oxygen species on ZnO surface and proposed a correlation between photon reactions and the antibacterial activity as follows. The electronic band structure of ZnO, as a semiconductor material, consists of a conduction band (CB) and a valence band (VB). Incident radiation with photons of energy greater than 3.37eV is immediately absorbed, thus the electrons move from the VB to the CB. This electron transfer initiates a series of possible photoreactions. As a result, positive holes (h^+) are formed in the VB, while free electrons are created within the CB. This positive hole (h^+), a direct oxidant and essential for the creation of reactive hydroxyl radicals ($OH^\bullet$), serves as principal oxidants in photo catalytic system. The electrons in the CB reduce oxygen, which is absorbed by the photo catalyst (Zhang, *et al*., 2012). The electron and hole interacts with water (H_2O) to produce $^\bullet OH$ and H^+. In addition, O_2 molecules (suspended within the mixture of bacteria and ZnO) yield superoxide anion (O_2^-), which reacts with H^+ to produce HO_2. Afterward, HO_2 interferes with electrons generating hydrogen peroxide ($^\bullet HO_2$); which combines with H^+ giving hydrogen peroxide (H_2O_2) molecules. These molecules are capable to enter the membrane where they either damage or kill the bacteria. H_2O_2 generation mainly relies on the surface of ZnO NPs to yield additional active molecules.

The researchers expressed the generated ROS by chemical equations as follows:

$$ZnO + h\nu \longrightarrow e^- + h^+ \quad \text{---------- (11)}$$

$$h^+ + H_2O \longrightarrow \cdot OH + H^+ \quad \text{..... (12)}$$

$$e^- + O_2 \longrightarrow \cdot O_2^- \quad \text{..... (13)}$$

$$\cdot O_2^- + H^+ \longrightarrow HO_2\cdot \quad \text{..... (14)}$$

$$HO_2\cdot + e^- + H^+ \longrightarrow H_2O_2 \quad \text{..... (15)}$$

The superoxides and hydroxyl radicals cannot penetrate into the membrane due to their negative charges. Thus, these species are found on the outer surface of the bacteria, by contrast, H_2O_2 molecules are able to pass through the bacterial cell wall, subsequently leading to injuries and destroy, and finally triggering cell death (Zhang, *et al.,* 2007). When ZnO NP kills or interacts with the cell membrane, the particles most probably stay firmly adsorbed at the surface of the left over / killed bacteria blocking additional antibacterial activity. Once ZnO nanoparticles are in the growth media, they will carry on releasing peroxides covering the entire surfaces of the dead bacteria. Therefore, this continuous peroxide release leads to higher bactericidal efficacy. In general, the electrostatic attraction between negatively charged bacterial cells and positively charged particles is crucial for the activity of nanoparticles bactericidal materials. This interaction not only inhibits the bacterial growth but also induces the reactive oxygen species generation, which leads to cell death (Zhang, *et al*., 2008).

2.6.2. Zinc ions (Zn^{2+}) release

One of the main proposed antibacterial mechanisms for ZnO NPs is the release of zinc ions in medium containing ZnO NPs and bacteria (Li, *et al*., 2011). The released Zn^{2+} has significant effect in the active transport inhibition as well as in the amino acid metabolism and enzyme system disruption. The researchers summarized that Zn^{2+} release mechanism affected by two main parameters:-(i) The physicochemical properties of the particles including porosity, concentration, particle size, and morphology. (ii) The chemistry of the media such as the pH, UV illumination, exposure time, and existence of other elements.

ZnO NPs are able to slow down the growth of bacteria due to disorganization of the bacteria membranes, which increases membrane permeability leading to accumulation of nanoparticles in the bacterial membrane and cytoplasmic regions of the cells. While the exact mechanisms of the antibacterial action have not yet been clearly understood, it has been advised that the rule of reactive oxygen species produced on the surface of the particles; zinc ion release, membrane dyesfunction, and nanoparticles internalization are the main reason of cell swelling (Ashe, 2011**)**.

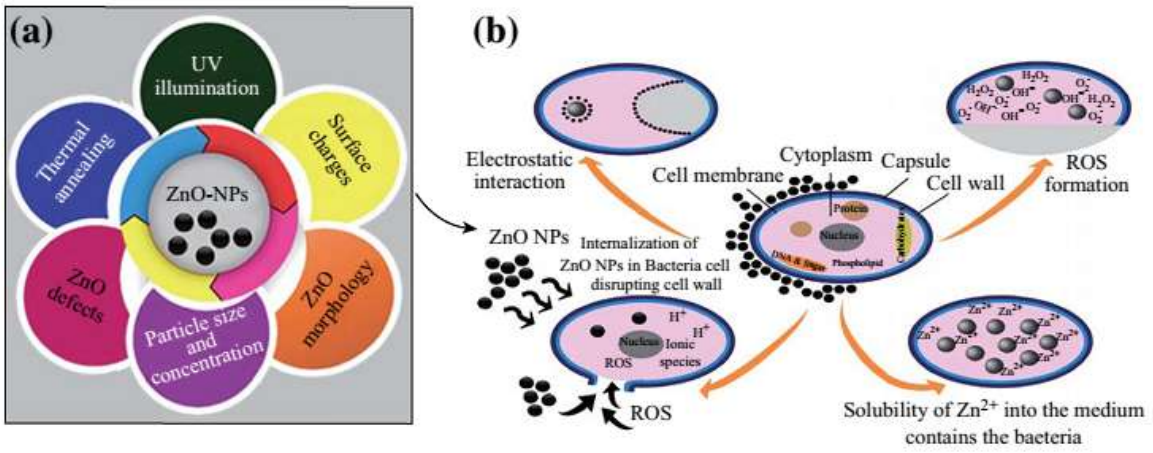

Figure 2: Correlation between the influence of essential ZnO NPs parameters on the antibacterial response and different possible mechanisms of ZnO NPs antibacterial activity (Amna. *et al*., 2015).

2.7 Characterization of ZnO Nanoparticles

2.7.1 Thermal gravimetric analysis (TGA)

Thermo gravimetric analysis or thermal gravimetric analysis (TGA) is a method of thermalanalysis in which the mass of a sample is measured over time as the temperature changes. This measurement provides information about physical phenomena, such as phase transitions, absorption and desorption; as well as chemical phenomena including chemisorptions, thermal decomposition, and solid-gas reactions (e.g. oxidation or reduction) (Liu and Yu, 2006). In a desired temperature range, if a species is thermally stable, there will be no observed mass change. Negligible mass loss corresponds to little or no slope in the TGA trace. The temperature

is generally increased at constant rate to incur a thermal reaction. The thermal reaction may occur under a variety of atmospheres including: vacuum, inert gas, oxidizing / reducing gases, corrosive gases, carburizing gases, vapors of liquids or "self-generated atmosphere"; as well as a variety of pressures including: a high vacuum, high pressure, constant pressure, or a controlled pressure.

2.7.2 XRD characterization of ZnO nanoparticles

X-rays were discovered by Wilhelm Rontgen, a German scientist in 1895. To generate x-rays, at least the following three things are required: a source of electrons, a means of accelerating the electrons at high speeds and a target material to receive the impact of the electrons and interact with them.A typical cathode element is Tungsten (W) with potential of 20-50 KV and the anodic material should be water cooled. The frequency (wavelength) depends on the anode material, usually Cu, Mo, or Co. Lines occur because bombarding electrons knock out e^- from K shell (n=1), which are filled by electrons in higher shells. Electrons falling from L shell (n = 2) give rise to K_a lines, whereas e^- from M shell (n = 3) give the Kb lines (Prellier, *et al*., 2003). Monochromatic radiation or a narrow range of wavelengths is required for X - ray diffraction. Typically, the K_a line is selected and the K_β line is filtered out by using a thin metal foil of the adjacent (Z – 1) element, for example Nickel filters K_β line of copper. A monochromatic beam of X - rays can also be selected by reflecting from a plane of a single crystal. The observed intensity is given by:

$$I = I_0 \, e^{-\mu t} \qquad \text{.. (1)}$$

Where, μ is a linear absorption coefficient andt is the path length through which the X - rays are moving (Yoshio, *et al.,* 2011).

The average crystallite size of ZnO nanoparticles is calculated using Debye Scherer formula according to Equation (2) (Sawai, 2003).

$$D=\frac{K\lambda}{\beta \cos\theta} \qquad \text{.................................... (2)}$$

Where D is average crystallite size, K is polarization factor (K = 0.94). λ is the X-ray wavelength used in XRD (Cu Ka line) (λ = 1.5406 ^{0}A), θ is the Bragg's angle (or scattering angle) in degrees and β is full width at half-maximum (FWHM) in radians, that is, broadening due to crystallite dimensions.Peak broadening may not only come from the size effect, but can also be due to strain in the particles. For non-uniform strain, the strain (∈) induced in powders due to crystal imperfection and distortion is calculated using the Williamson-Hall formula (3):

$$\in = \frac{\beta}{4 \tan\theta} \qquad \ldots\ldots\ldots\ldots\ldots\ldots\ldots\ldots\ldots\ldots\ldots\ldots\ldots\ldots (3)$$

From Equations 2 and 3, it is confirmed that the peak width from crystallite size varies as 1/cosθ strain varies with tanθ.

Assuming that the crystallite size and strain contributions to line broadening are independent to each other and both have a Cauchy-like profile, the obtained line breadth is simply the sum of Equations 2 and 3, which results Equation(4):

$$\beta = \frac{K\lambda}{D \cos\theta} + 4 \in \tan\theta \qquad \ldots\ldots\ldots\ldots\ldots\ldots\ldots\ldots\ldots\ldots\ldots\ldots (4)$$

By rearranging the above equation, one can get:

$$B \cos\theta = \frac{K\lambda}{D} + 4 \in \sin\theta \qquad \ldots\ldots\ldots\ldots\ldots\ldots\ldots\ldots\ldots\ldots\ldots\ldots (5)$$

The above equations are Williamson–Hall (W–H) Equations (4) and (5) (Cullity and Stock, 2001).

The micro strain (∈) and crystallite size (D) is also calculated from XRD data using Williamson–Hall (W–H) plot with following relation (Cullity and Stock, 2001):

$$\frac{\beta \cos\theta}{\lambda} = \frac{1}{D} + \in \frac{\sin\theta}{\lambda} \qquad \ldots\ldots\ldots\ldots\ldots\ldots\ldots\ldots\ldots\ldots\ldots\ldots (6)$$

The strain (∈) is determined from the slope of line by using W-H plot (plot of β cosθ versus 4sinθ).

The lattice parameters 'a' and 'c' and the spacing, '$d_{h\ k\ l}$', for wurtzite structure of ZnO have been calculated according to Eqns. (7) and (8).

$$a = \sqrt{\frac{1}{3}}\frac{\lambda}{\sin\theta} \quad \text{and} \quad c = \frac{\lambda}{\sin\theta} \qquad \ldots\ldots\ldots\ldots\ldots\ldots\ldots (7)$$

$$d_{h\,k\,l} = \frac{ac}{2}\sqrt{\frac{3}{c^2(h^2 + hK + K^2) + 3\,\frac{(al)^2}{4}}} \qquad \ldots\ldots\ldots\ldots\ldots\ldots\ldots (8)$$

The inter planar spacing can be calculated from the Bragg's law according to Equation (9).

$$2d\sin\theta = n\lambda \qquad \text{where, } n = 1, 2, 3, \text{---} \qquad \ldots\ldots\ldots\ldots\ldots\ldots (9)$$

Where n is the order of diffraction (usually n = 1), λ is the X-ray wavelength, d is distance between adjacent planes in the lattice and θ is the incident angle of the X-ray beam (or Bragg's angle).

2.7.3 Fourier-transform infrared spectroscopy (FT-IR)

Fourier-transform infrared spectroscopy (FT-IR) is an effective method to reveal the composition of products, information on the vibrational and rotational modes of motion of a molecule and hence an important technique for identification and characterization of a substance. FT-IR is a technique used to obtain an infraredspectrum of absorption or emission of a solid, liquid or gas. It is the preferred method of infrared spectroscopy. In infrared spectroscopy, IR radiation is passed through a sample. Some of the infrared radiation is absorbed by the sample and some passed through or transmitted. The resulting spectrum represents the molecular absorption and transmission, creating a molecular fingerprint of the sample. Like a fingerprint, no two unique molecular structures produce the same infrared spectrum. This makes infrared spectroscopy useful for several types of analysis. Therefore, from FT-IR one may obtain both qualitative and quantitative material's information (Stuart, 2004). Usually most of the metals and its oxide, give the FT-IR peaks at lower wave number ranging from 400 to 800 cm^{-1}. FT-IR spectra of samples of ZnO nanoparticles are generally influenced by the particle size and morphology.

2.7.4 Scanning electron microscopy (SEM)

The Scanning electron microscopy (SEM) is routinely used to generate high-resolution images of shapes of objects.The scanning electron microscope (SEM) uses a focused beam of high-energy electrons to generate a variety of signals at the surface of solid specimens. The signals that derive from electron sample interactions reveal information about the sample including external morphology (texture), chemical composition, and crystalline structure and orientation of materials making up the sample. The SEM is also capable of performing analyses of selected point locations on the sample; this approach is especially useful in qualitatively or semi-quantitatively determining chemical compositions (using EDS), crystalline structure, and crystal orientations (using EBSD).

2.7.5 Reflectance, transmittance, and absorption

Reflectance (ρ) is the amount of flux reflected by a surface, normalized by theamount of flux incident on it. Transmittance (τ) is the amount of flux transmitted bya surface, normalized by the amount of flux incident on it. Any flux not reflectedor transmitted is absorbed (α). Conservation of energy requires that:

$$\rho + \tau + \alpha = 1 \qquad \ldots\ldots\ldots\ldots\ldots\ldots\ldots\ldots\ldots\ldots\ldots \text{(10)}$$

But, for a solid substance:

$$\rho + \tau = 1 \qquad \ldots\ldots\ldots\ldots\ldots\ldots\ldots\ldots\ldots\ldots\ldots \text{(11)}$$

3. MATERIALS AND METHODS

Pure and analytical grade chemicals were used in all experiments for the synthesis of ZnO nanoparticles and media preparation for growth of bacterial cells.

3.1 Experiment Site

The experiments for synthesis of ZnO nanoparticles, the TGA and XRD characterizations of the synthesized samples of ZnO NPs, and evaluation of antibacterial activities of ZnO nanoparticles against selected pathogenic bacteria were carried out at the Adama Science and Technology University, Ethiopia. The FT-IRcharacterization of synthesized samples of ZnO nanoparticles was conducted at Addis Ababa University, in Chemistry laboratory and that of SEM, EDX and UV-vis characterization at India.

3.2 Apparatus and Instruments

3.2.1 Apparatus

The laboratory apparatus that were used for this study are different sized glasswares, beakers, volumetric and erlenmeyer flasks, measuring cylinders, pipettes, droppers, funnels, crucible dish, Whatman filter paper number one, spatula and tong .

3.2.2 Instruments

The instruments used in this study were FT-IR, XRD, SEM, EDX, and UV-vis modern techniques, reciprocating shaker, muffle furnace, magnetic stirrer, mortar and pestle, hot air oven, digital balance, hot heating plate and incubator shaker.

3.3 Chemicals and Solvents

The chemicals and solvents used in this research work were Zinc acetate dihydrate ($[Zn(CH_3COO)_2.2H_2O]$, MW=219.5 g/mo, 98 %from Ranchem Industry & Trading), Zinc nitrate hexahydrate ($[Zn(NO_3)_2.6H_2O]$, MW=297.49 g/mo, 96% laboratory reagent), Sodium hydroxide ([NaOH], MW=39.99971 g/mol, 99.8% from Ranchem Industry & Trading),

zinc chloride hexahydrate ([$ZnCl_2.6H_2O$], MW=244.3777 g/mol, 99.9% "UNI-CHEM" Chemical Reagents), dimethyl sulphoxide ([C_2H_6OS], MW = 78.14 g/mol, 99.5%), Ethanol absolute (99.9% from Ranchem Industry & Trading) and distilled water, as solvents.

3.4 Synthesis of ZnO nanoparticles using solochemical method

The precursor and precipitant chemicals for the preparation of ZnO nanoparticles were zinc nitrate hexahydrate, sodium hydroxide, zinc chloride hexahydrate and zinc acetate dihydrate. In this study, solochemical method was used for the preparation of ZnO nanoparticles (Figure 3)

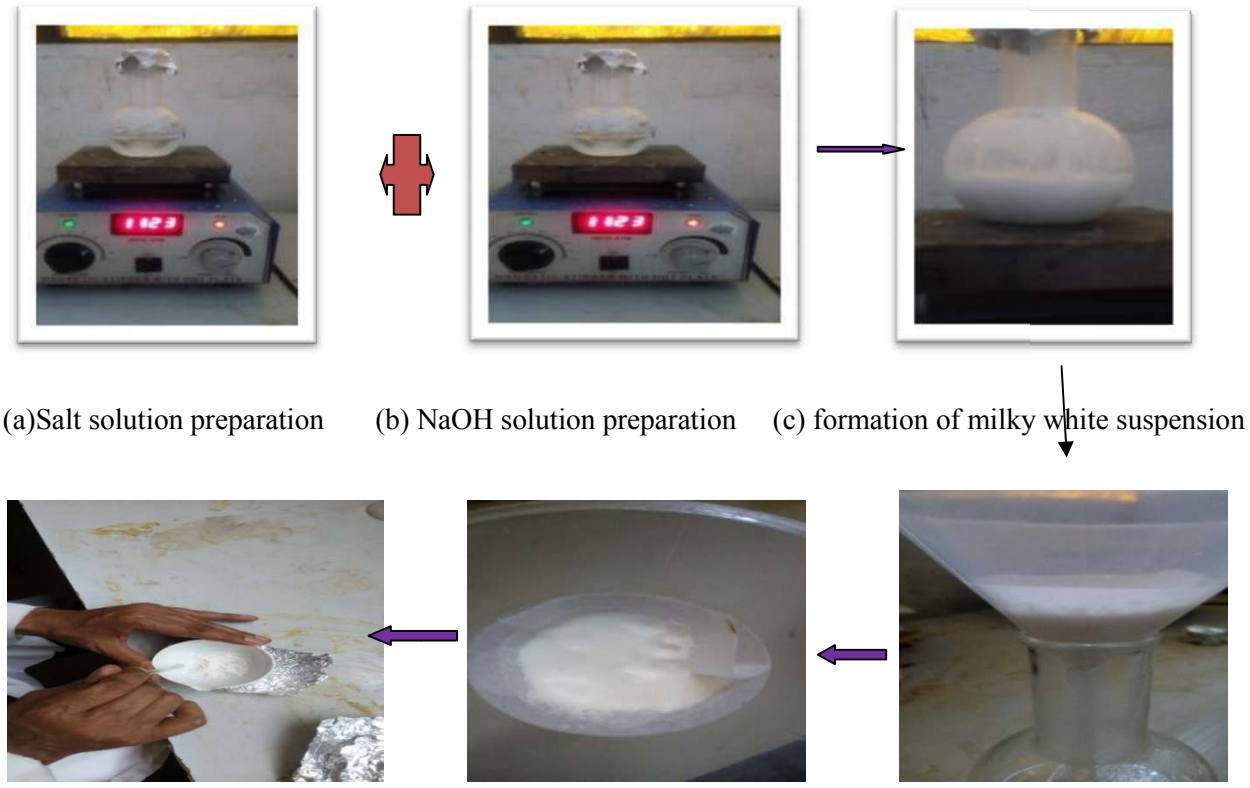

(a)Salt solution preparation (b) NaOH solution preparation (c) formation of milky white suspension

(f) Synthesized ZnO NPs (e) Prepared ZnO powder (d) filtration and washing

Figure 3: Pictorial representation of ZnO nanoparticles synthesis using solochemical method.

3.4.1 Synthesis of ZnO NPs using Zinc nitrate hexahydrate [$Zn(NO_3)_2.6H_2O$]

The synthesis procedures for ZnO nanoparticles preparation from $Zn(NO_3)_2.6H_2O$ precursor were conducted according to the procedures developed by(Marivone, *et al.,* 2011). About 15 g of

$Zn(NO_3)_2.6H_2O$ was dissolved in 100 ml of distilled water in a beaker and stirred for 25 minutes using magnetic stirrer. The resulting solution was heated under constant stirring at the reaction temperature of 70°C. Subsequently, 4 g of NaOH was also dissolved in 30 ml of distilled water in a separate beaker and stirred for 10 minutes. After this, a solution of NaOH was slowly added drop by drop into the beaker containing $Zn(NO_3)_2.6H_2O$ solution under stirring condition. The suspension formed with the dropping of NaOH alkaline aqueous solution to the $Zn(NO_3)_2.6H_2O$ solution was kept stirred for two hours at the temperature of 70°C in order to hydrolyze zinc nitrate solution into zinc hydroxide. The mixed solution was settled under normal air condition for few hours, and filtered using Whatman filter paper no 1 and washed by distilled water and then by absolute ethanol sequentially.The washing procedure was repeated several times in order to remove the residual impurities present in the sample. The final white products were dried at 160°C in hot air oven for 3 1/2 hours to remove volatile substances and for the conversion of $Zn(OH)_2$ into ZnO **(**Marivone, *et al.,* 2011). Finally, the obtained nanosized ZnO powder particles were calcined at 300°C for 5 hours in a muffle furnace and then, were grinded using mortar and pestle.

In this process, the reaction of Zn^{2+} ions and sodium nitrate proceeds as shown in the Equations (16, 17):

$$Zn(NO_3)_{2(aq)} + 2NaOH_{(aq)} \xrightarrow{70°C} Zn(OH)_2\downarrow + 2NaNO_{3\,(aq)} \quad \ldots\ldots\ldots\ldots\ldots (16)$$

$$Zn(OH)_2\downarrow + 2NaNO_{3(aq)} \longrightarrow Zn(OH)_2 \quad \ldots\ldots\ldots\ldots\ldots (17)$$

The formed precipitant decomposes upon calcining to ZnO as represented in Equation (18).

$$Zn(OH)_2 \xrightarrow{300°C} ZnO + H_2O \quad \ldots\ldots\ldots\ldots\ldots (18)$$

The calcinated and uncalcinated samples of ZnO NPs synthesized from $Zn(NO_3)_2.6H_2O$ at the reaction temperatures of 300^{o}C are designated as S1 and US1(US1 =S0), respectively.

3.4.2 Synthesis of ZnO NPs using zinc chloride hexahydrate [$ZnCl_2.6H_2O$]

The synthesis procedures for zinc oxide nanoparticles preparation using$ZnCl_2.6H_2O$precursor were conducted according to the procedures developed (Parthsarathi and Thilagawathi, 2011). About 20 g of zinc chloride hexahydrate was dissolved in 100 ml of distilled water in a beaker and stirred for 45 minutes using magnetic stirrer at the temperature of 90°C. Similarly, 7.3 g of NaOH was dissolved in 100 ml of distilled water in a separate beaker and stirred for 20 minutes. 58 ml solution of sodium hydroxide was added to the beaker containing $ZnCl_2.6H_2O$ solution with constant stirring at 90°C. The aqueous solution was turned into a milky white colloid without any precipitation. The reaction was allowed to proceed for 2 hours after complete addition of sodium hydroxide. The solution was allowed to settle and filtered with Whatman filter paper no 1, and washed several times using distilled water first and then by 99.9% ethanol in order to remove impurities. The filtered sample was allowed to dry in oven at 160°C for 7 hours and calcinated at 600°C, 700°C and 800°C each for 2 hours in a muffle furnace. Finally, the material was grinded using mortar and pestle.The samples of ZnO NPs synthesized from $ZnCl_2.6H_2O$ at the calcination temperatures of 600^oC, 700^oC and $800^oC$are designated as S22, S2 and S4, respectively.

The schematic view of zinc Oxide nanoparticles preparation flow chart using the prepared solutions of $ZnCl_2.6H_2O$ and NaOH by solochemical method is shown as:

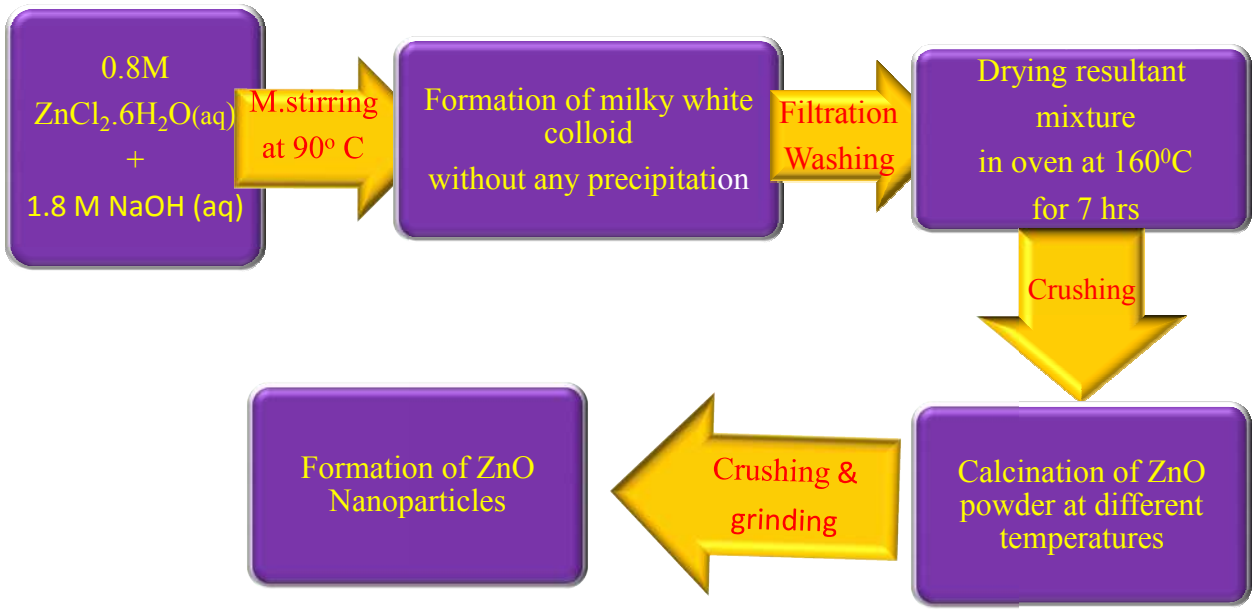

Figure 4: Schematic preparation route of zinc oxide NPs from $ZnCl_2.6H_2O$ precursor by solochemical processing.

3.4.3 Synthesis of ZnO NPs using zinc acetate dihydrate [$Zn(CH_3COO)_2 .2H_2O$]

The synthesis of zinc oxide nanoparticles was conducted according to the procedures developed (Rajneesh, *et al*., 2012). In present work, thermal decomposition method is applied for the preparation of high-purity ZnO nanoparticles by placing and decomposing zinc acetate dihydrate (15g) into a crucible and calcinated at 400℃ for two reaction times 12 hrs and 2½ hrs in a muffle furnace without any special atmospheric condition. Finally, the material was grinded using mortar and pestle and put ready for characterization and antibacterial application.The samples with reaction times of 2½ hrs and 12 hrs are designated as S32 and S3, respectively.

3.5 Methods of Characterization of ZnO Nanoparticles

3.5.1 Thermal gravimetric analysis (TGA)

Thermal gravimetric analysis (TGA) was carried out using a simultaneous DTA-TG apparatus (DTG-60H, Shimadzu Co., Japan) to predict the calcination temperature of the synthesized samples of ZnO. Approximately 16.592 mg of the uncalcinated sample of ZnO nanoparticles prepared from zinc chloride hexahydrate precursor and 17.465 mg of uncalcinated sample of ZnO nanoparticles obtained from zinc nitrate hexahydrate were placed separately in a platinum crucible on the pan of the microbalance and heated from 25^0C to 1000°C, using Al_2O_3 as inert material.

3.5.2 X-ray diffraction (XRD) method

The X-ray powder diffraction patterns of the ZnO nanoparticles were recorded using X-ray Diffractometer(Bruker D8 Advance Diffractometer) equipped with nickel filtered Cu-Kα radiation (λ = 1.5406 ^{0}A = 0.15406 nm) operating at 40 KV and 30mA. The data have been collected in the scan range (2θ) from 10-80° at Adama Science and Technology University, Department of Material Science and Engineering. The average crystallite size of ZnO nanoparticles is estimated by using Debye Scherer formula indicated in equation (2):

$$D = \frac{K\lambda}{\beta \cos\theta} \quad \text{..... (2)}$$

Where D is average crystallite size, K is polarization factor (K = 0.94),λ is the X-ray wavelength used in XRD (λ = 1.5406 ^{0}A), θ is the Bragg's angle in degrees and β is full width at half maximum (FWHM) in radians.

3.5.3 Fourier transform infrared spectroscopy (FT-IR) method

The vibrational phonon and surface functional groups of ZnO NPs were characterized by Fourier transform infrared spectroscopy (Perkin Elmer, 65) in the wave number region of 4000-400 cm^{-1} according to the procedures reported (Suhandro and Rosari, 2012) using the KBr pellet. The sample pellet for FT-IR was prepared by mixing KBr and ZnO NPs under ratio of 200:1. Then,

the FT-IR spectra measurements of the ZnO nanoparticles were performed by putting the powder ZnO nanoparticles on KBr pellet.

3.5.4 Scanning electron microscopy (SEM) method

In this research work, the morphological feature of ZnO NPs was determined by Scanning electron microscopy using electron beam energy of 10 KV and 15 KV. The ZnO nanoparticles powder is mounted on a sample holder followed by coating with a conductive metal. Then, the sample was scanned with focused fine beam of electrons. The surface characteristics of the sample were obtained from the secondary electrons emitted from the sample surface

3.5.5 Energy dispersive X- ray spectroscopy

The chemical composition of the synthesized zinc oxide nanoparticles was estimated by energy-dispersive X-ray spectroscopy (EDX). This technique is an analytical technique used to determine the elemental analysis or chemical characterization of a sample through interaction in between sample and source of X-ray excitation. At rest, every atom has definite arrangement of electron in discrete energy levels around the nucleus. When high energy beam of radiation hit the sample (matter), it may excite an electron from inner shell and create a hole over there. To compensate this vacancy an electron**s** from outer shell migrate to inner shell, while the difference in energy between outer and inner shell may be generated in the form of X-ray. As, every element has a definite electronic arrangement, when the sample is being hit with high energy electromagnetic radiations it will generate characteristic X-ray this is like fingerprint for every element. The number and energy of X-rays emitted from sample can be measured by a detector.

3.5.6 UV-Visible spectroscopy

The optical characterization of ZnO NPs was carried out using UV-Vis Spectroscopy (Perkin–Elmer lambda 950 UV/VIS/NIR/ spectrometer) in the wave length region of 200 nm - 800 nm. First a dimethyl sulfoxide solvent was inserted in a 1 cm cuvette as a reference and the dimethyl sulfoxide solution and ZnO nanoparticles was placed in the second cuvette compartment for UV – Vis absorbance / reflectance measurement. Bandgap energy (Eg) of the synthesized ZnO NPs was obtained using the relation (El-Kemary, *et al.*, 2010).

$$Eg\ (eV) = \frac{1240}{\lambda} \quad \ldots\ldots (12)$$

Where Eg is band gap energy in electron volts and λ is wavelength (nm) corresponding to absorption maxima (or reflectance minima).

3.6 Method for Testing Antibacterial Activity of ZnO Nanoparticles

Different methods have been adopted for the assessment and investigation of antibacterial activity in **vitro**. These methods include disk diffusion, broth dilution, agar dilution, agar well diffusion and the micro titer plate-based method. In this work, the antibacterial activity of the zinc oxide nanoparticles on gram-positive ((*Staphylococcus aureus* (ATCC 25923) and *Basilius subtilis* (ATCC 6633)) and gram-negative ((*Escherichia coli* (ATCC 25922) and *Pseudomonas aeruginosa* (ATCC 7553)) bacteria was tested by agar well diffusion method according to the procedures reported (Sawai, 2003).

The materials used for antibacterial activity of zinc oxide nanoparticles are Nutrient broth 1.3 g, Nutrient agar 5.6 g, Agar-agar 0.5 g, petriplates, antibiotic discs, cotton swabs, zinc oxide nanoparticles samples, Escherichia coli, Pseudomonas aeruginosa, Basilius subtilis and Staphylococcus aureus. The selection of the organisms was based on their roles for causing infections such as diarrhea in both children and early-weaned piglets.

3.6.1 Preparation of inoculums

Nutrient broth (1.3 g in 100 ml distilled water (Robert, 2003) was prepared in 8 conical flasks (1^{st}, 2^{nd}, 3^{rd}, 4^{th}, 5^{th}, 6^{th}, 7^{th} and 8^{th}). These conical flasks clinically isolated strain of Staphylococcus aureus (1^{st} and 2^{nd}), Escherichia coli (3^{rd} and 4^{th}), Basilius subtilis ($5^{th}$and 6^{th}) and Pseudomonas aeruginosa (7^{th} and 8^{th}) were inoculated. These bacterial cultures inoculated in nutrient broth were kept on rotary shaker for 24 hours at 100 revolutions per minutes (r.p.m).

3.6.2 Inoculation of test plate

Nutrient agar is prepared (5.6 g nutrient agars, 0.5g Agar- agar in100 ml distilled water) (Rezende, *et al.,* 2009). The agar suspension within 15 minutes is used to inoculate plates by

dipping a sterile cotton-wool swab into the suspension and remove the excess by turning the swab against the side of the container (Figure 5). Then inoculums were spread evenly over the entire surface of the plate by swabbing in three directions.Then, the plate was allowed to dry before applying antibiotic to discs.

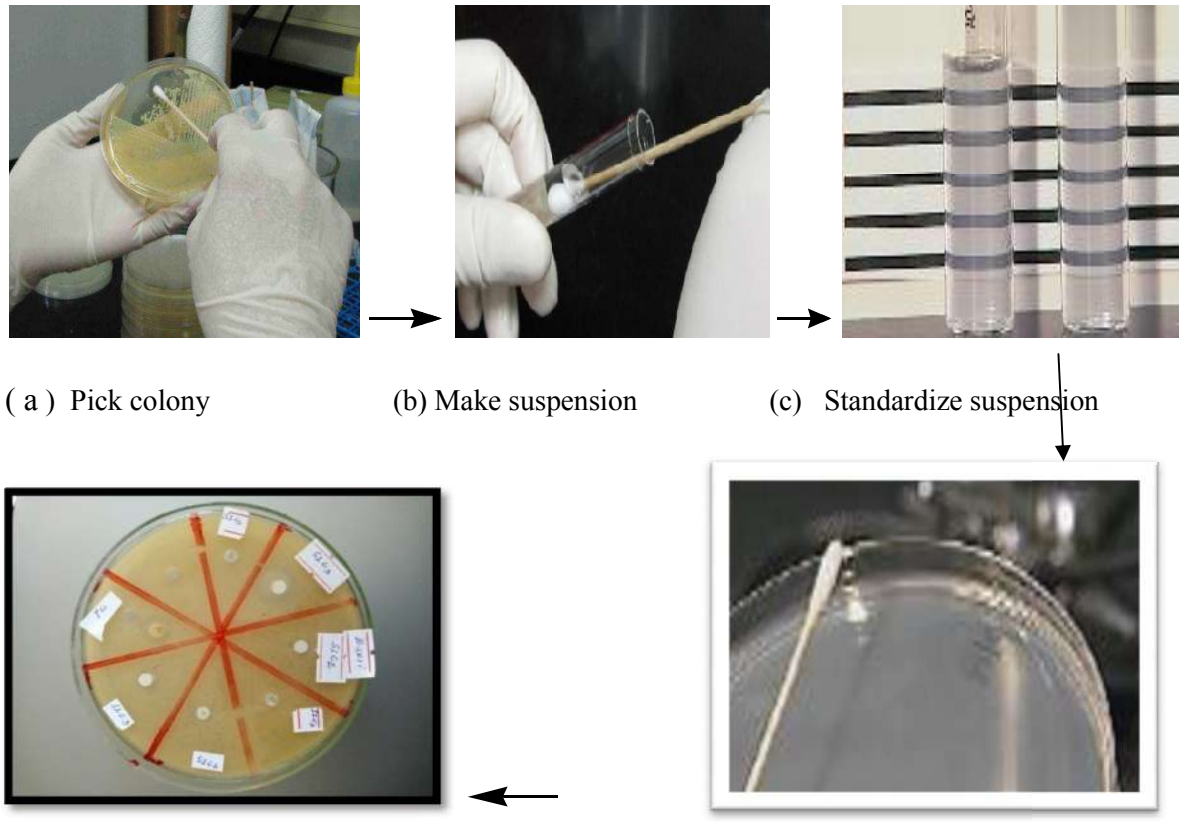

(a) Pick colony (b) Make suspension (c) Standardize suspension

(e) Apply agar well diffusion and Read results (d) Inoculate bacteria lawn

Figure 5: Procedures for anti-bacterial activity testing by agar well diffusion method.

3.6.3 Agar well diffusion method for anti-bacterial activity test

Antibacterial tests were carried out by the agar well diffusion method using the suspension of bacteria spread on nutrient agar. Then, antibacterial activity of synthesized ZnO nanoparticles was tested against gram- negative (*Pseudomonas aeruginosa* and *Escherichia coli)* and gram-positive (*Staphylococcus aureus* and *Basilius subtilis*) bacteria. The selection of the test micro-organisms was based on their roles for causing infections such as diarrhea in both children and early-weaned piglets. The Mueller-Hinton agar was used as a nutrient medium for initiating the

growth of bacterial by swabbing each test strain on it. The standard antibiotic drug gentamyicin (30μg) and the blank without inoculation were used as positive control (Pc) and negative control (Nc), respectively. Subsequently, about 100 mg, 200 mg and 300 mg of each calcinated samples of ZnO nanoparticles synthesized from the salt precursors was dispersed separately in 10 ml of dimethyl sulfoxide (DMSO) and stirred for 2 hrs using magnetic stirrer. Then, the wells were made on each Petri- plates by using sterile cork borer having a diameter of 6 mm. About 150 μL of each sample of the three different prepared ZnO nanoparticles solutions and positive control (Pc) were poured into wells on all plates with the help of micropipette. In addition to these; the antibacterial activity of uncalcined sample of ZnO NPs obtained from $Zn(NO_3)_2.6H_2O$ was tested using these bacterial strains. The plates were then turned upside down and incubated at 37^0C for 24 hrs in an incubator (Figure 6). Finally, after incubation, the zones of inhibition formed around the wells against the test organisms were calculated by measuring the diameter of the inhibition zone around the well in millimeters (mm) by using a ruler and recorded, including the well diameter. The readings were taken in three different fixed directions in all three replicates, and the average values were tabulated.

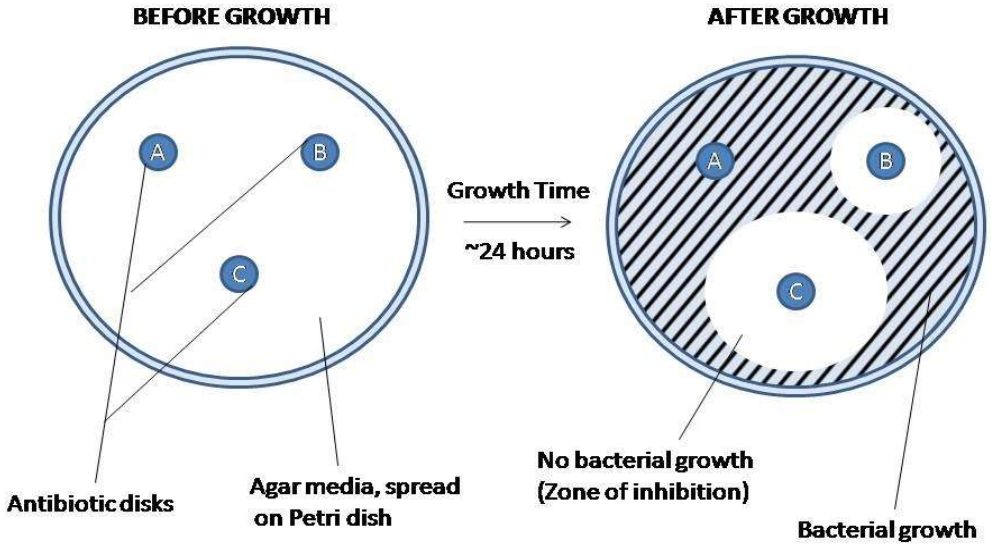

Figure 6: Pictorial representation of the growth of bacteria during incubation technique.

4. RESULTS AND DISCUSSION

4.1 Characterization of Zinc oxide Nanoparticles

The crystallinity of ZnO powder, morphological features, chemical composition, thermal behavior and vibrational phonons of ZnO NPs were characterized by X-ray Diffractometer (XRD), Scanning Electron microscopic (SEM), Energy Dispersive X- Ray Spectroscopy **(**EDX), Thermal Gravimetric Analysis (TGA) and Fourier Transform Infrared Spectroscopy (FT-IR), respectively.

4.1.1 Thermal gravimetric analysis (TGA)

The uncalcinated samples of ZnO nanoparticles solochemically synthesized from zinc nitrate hexahydrate and zinc chloride hexahydrate precursors were characterized through analysis of their weight loss by Thermal Gravimetric Analysis (TGA) and Differential Thermal Analysis (DTA) techniques. TGA curve shows weight loss of the sample whereas DTA curve indicates the energy gain or loss during the process. Figure 7 shows the thermo gravimetric analysis (TGA) and differential thermal analysis (DTA) of the uncalcined sample of ZnO nanoparticles obtained from zinc chloride hexahydrate. According to Figure 7, thermo gravimetric analyzer showed that there is 7.275 % weight loss (-1.207mg) from 25℃ up to 200℃, 9.456 % loss of weight from 200-500℃and 11.319 % from 500 ℃ up to 700℃. After 700℃, the percent weight loss of the sample (0.47%) is relatively very small and these nanoparticles are thermally stable at this temperature and hence this was the calcination temperature of the given sample (Fig.7). In general, the thermo gravimetric analysis is used to predict the possible calcination temperature of sample of ZnO NPs synthesized from a precursor. Thus, for comparative study, 600^0C, 700^0C and 800^0C were used as calcination temperatures of samples of ZnO nanoparticles synthesized from zinc chloride hexahydrate precursor.

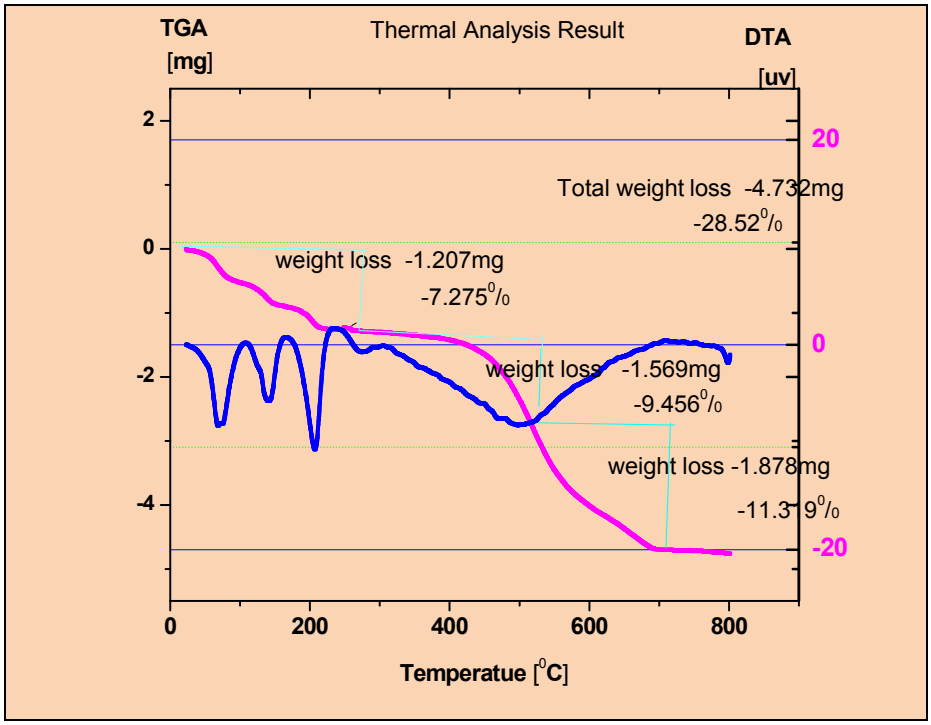

Figure 7: Thermal analysis result for uncalcinated samples of ZnO NPs obtained from zinc chloride hexahydrate.

Figure 8 shows the thermo gravimetric analysis (TGA) and differential thermal analysis (DTA) of the uncalcined sample of ZnO nanoparticles synthesized from zinc nitrate hexahydrate (US1). In this Figure, thermo gravimetric analyzer showed that there is 3.309% weight loss (-0.578mg) from 25℃to 800℃, 10.53% loss of weight from 800 ℃ up to 1000℃ and a total of 13.793% loss of weight during this experiment. Probable around 300°C, there is negligible mass loss which corresponds to little or no slope in the TGA trace. Thus, 300℃ can be used as the calcination temperatures of sample of ZnO NPs prepared from zinc nitrate hexahydrate (Fig.8).

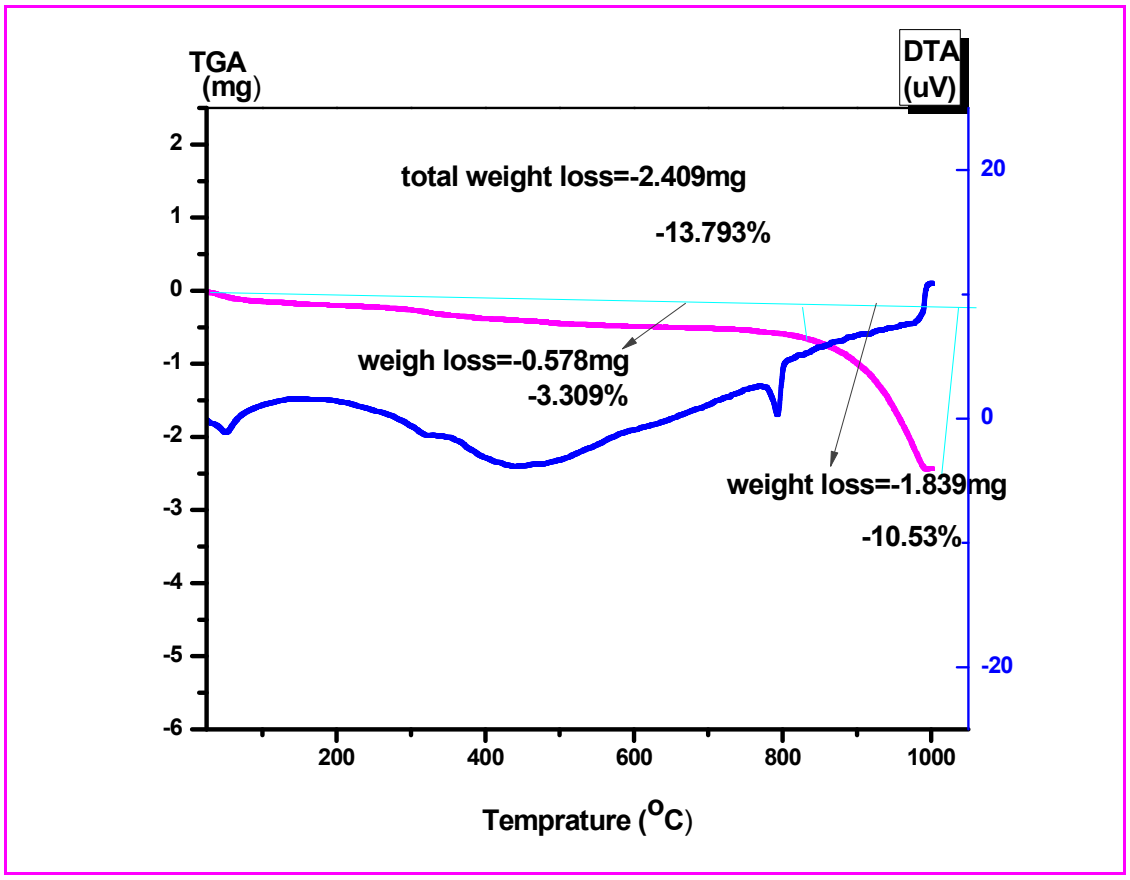

Figure 8: Thermal analysis result for uncalcinated sample of ZnO NPs obtained from zinc nitrate hexahydrate.

4.1.2 X-ray diffraction (XRD) analysis of ZnO nanoparticles

Figure 9 and 10 show the XRD patterns of ZnO nanoparticles synthesized from three salts precursors of zinc by using the solochemical method.

The crystalline structure of the calcinated sample of ZnO nanoparticles (S1) prepared at 70°C by chemical reaction between 3M NaOH and 0.5M $Zn(NO_3)_2.6H_2O$ solution was analyzed by X-ray Diffractometer with CuKα radiations (λ = 1.5406 Å) in the range of 10˚ to 80˚ at room temperature (Figure 9). The 2θ variation was employed with a 0.02 degree step and a time step o.40 second at the current of 30 mA and voltage of 40 KV by depositing about 0.5 g of the dried particles of each sample randomly onto a plexi-glass sample container.

The X-ray diffraction peaks at scattering angles (2θ) around 31.73, 34.40, 36.23, 47.52, 56.56, 62.84, 66.31, 67.93,and 69.06 corresponds to the reflection from (100), (002), (101), (102), (110), (103), (200), (112) and (201) crystal planes for the sample of ZnO NPs obtained from $Zn(NO_3)_2.6H_2O$) as precursor, respectively. These confirm the formation of a high purity hexagonal wurtzite crystalline structure of ZnO, which is in agreement with the data from JCPDS, Card No.00-036-1451 (C. Chen, 2007) with unite cell parameters: a = b = 3.2498 Å and c = 5.2066 Å.

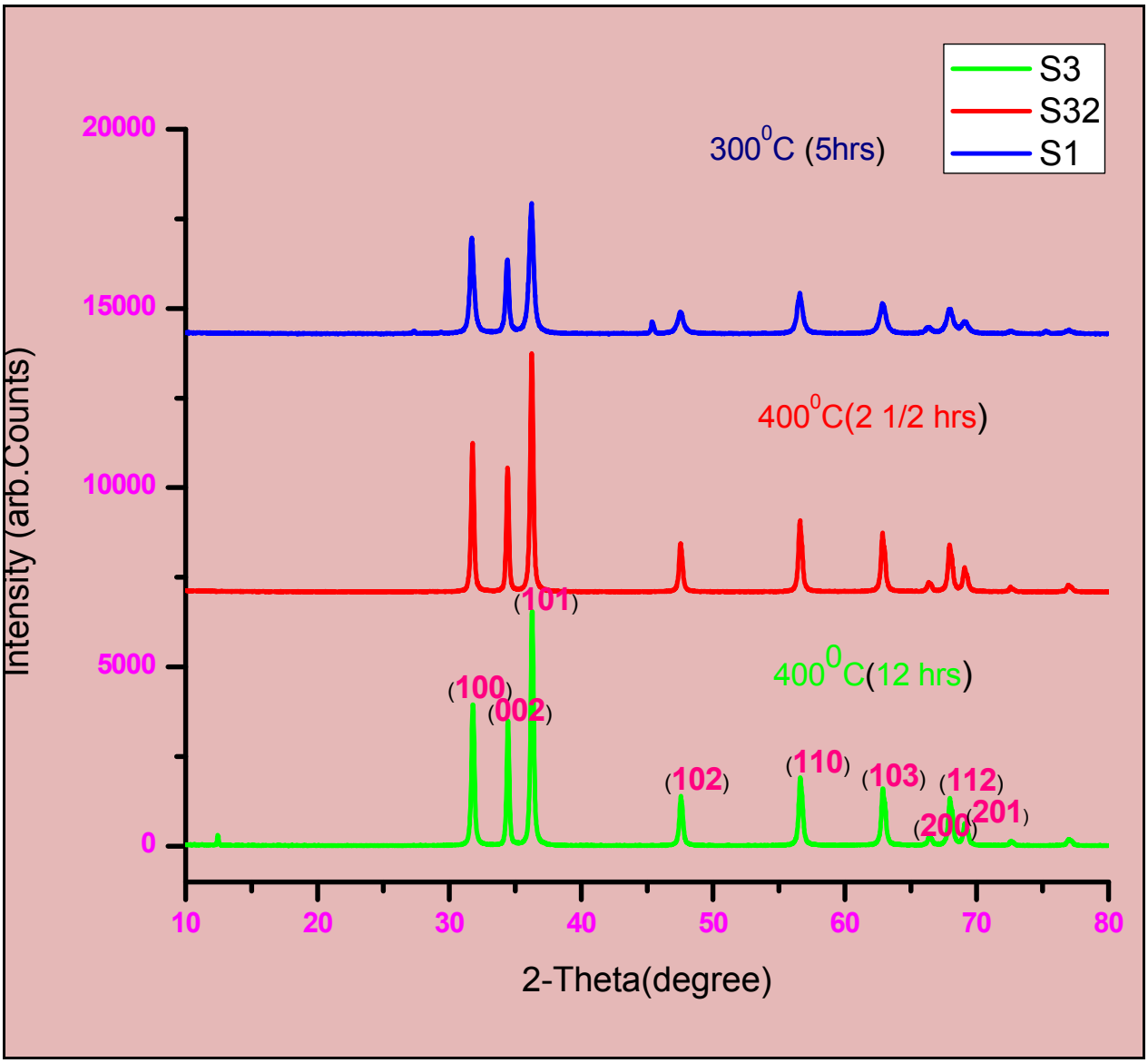

Figure 9: XRD patterns of samples of ZnO NPs synthesized using zinc nitrate hexahydrate and zinc acetate dihydrate at different calcination temperatures and times.

The 2**θ** values of (100), (002), (101), (102), (110), (103), (200), (112) and (201) lines and other parameters for each sample of ZnO NPs synthesized from the three salts' precursors of the crystal planes in Figures 9 and 10 are summarized in the Tables 1, 2 and 3 at different conditions.

Table 1: The XRD parameters and average crystallite size of ZnO NPs synthesized using zinc nitrate hexahydrate as precursor at calcination temperature of 300^0C for 5 hrs.

Sample ID & its calcination temperature	Miller Indices (h k l)	2θ (degree)	d-spacing (A)	FWHM=β (A)	Strain	Grain Size (nm)	Lattice Parameters (nm)	
							a	c
S1	(100)	31.7279	2.81796	0.3573	0.00549	24.16	0.325	0.5633
	(002)	34.4049	2.60457	0.3049	0.0043	28.49	0.301	0.5208
300°C	(101)	36.2312	2.47736	0.3859	0.00515	22.64	0.286	0.4953
3 ½ hrs	(102)	47.5228	1.91175	0.4825	0.00478	18.79		
	(110)	56.5593	1.62588	0.4437	0.00353	21.24		
	(103)	62.8444	1.47754	0.4805	0.00343	20.23		
	(200)	66.3106	1.40846	0.4833	0.00323	20.51		
	(112)	67.9335	1.37871	0.5048	0.00327	19.82		
	(201)	69.0585	1.35897	0.5394	0.00342	18.68		
		Average			**0.00407**	**21.62**	**0.304**	**0.526**

From Tables 1 and 2, quantitative analysis revealed that the powder consists of single phase ZnO with the calculated average lattice parameters: a = 3.04 Å, c = 5.26 Å for sample S1, a = 3.07 Å, c = 5.17 Å for sample S3, a = 3.04 Å, c = 5.26 Å for sample S32. This illustrates that the XRD patterns of samples of ZnO NPs obtained from Zinc nitrate hexahydrate and Zinc acetate dihydrate reveal that all diffraction peaks of samples are sharp and correspond to the characteristic peaks of hexagonal wurtzite structure of zinc oxide NPs by comparing with the data from JCPDS card 00-036-1451with lattice parameters (a = 3.2498 Å and c = 5.2066 Å)

(Srinivasa, 2015). However, the diffraction peaks of these samples are considerably broader than those presented by the JCSD pattern.

Table 2: The XRD parameters and average crystallite sizes of samples of ZnO NPs synthesized using zinc acetate dihydrate at two different calcination times.

Sample ID &its calcination temperature	Miller Indices (h k l)	2θ (degree)	d-spacing (A)	FWHM=β (A)	Grain Size (nm)	Lattice Parameters(nm) a	c
S3	(100)	31.806	2.81123	0.25	34.54	0.33	0.562
	(002)	34.462	2.60041	0.2143	40.54	0.3	0.4952
400°C	(101)	36.289	2.47357	0.2475	35.28	0.29	0.495
12 hrs	(102)	47.575	1.90979	0.2618	34.56		
	(110)	56.629	1.62404	0.2682	35.15		
	(103)	62.894	1.47649	0.2687	36.19		
	(200)	66.416	1.40647	0.2632	37.68		
	(112)	67.982	1.37785	0.2774	36.09		
	(201)	69.117	1.35796	0.2987	33.69		
		Average			**35.97**	**0.307**	**0.517**
S32	(100)	31.776	2.81384	0.2451	35.18	0.325	0.564
	(002)	34.434	2.60242	0.2155	40.32	0.3	0.52
400°C	(101)	36.26	2.47548	0.2476	35.27	0.286	0.495
2 1/2 hrs	(102)	47.546	1.91087	0.2547	35.56		
	(110)	56.601	1.62477	0.2621	35.99		
	(103)	62.869	1.47703	0.2681	36.27		
	(200)	66.388	1.40701	0.2831	35.01		
	(112)	67.954	1.37834	0.2804	35.71		
	(201)	69.09	1.35842	0.2793	36.1		
		Average			**36.16**	**0.304**	**0.526**

From literature, such broadening is a typical feature of nanometer-scale materials.According to XRD analysis for samples of S1, S3and S32, almost no peaks of any other phase were detected as shown in the Figure 9 (S1, S3& S32). The absence of extra peaks, which could be related to impurities, indicates that ZnO NPs samples produced from $Zn(NO_3)_2.6H_2O$ and $Zn(CH_3COO)_2.2H_2O$) precursors have high pure phases (Figure 9). In addition to this, the XRD pattern may show the sharp peaks and a high crystallinity of sample levels of ZnO nanoparticles obtained from all these samples particularly with the first three strongest peaks of the diffraction angles (2θ) at (100), (002) and (101) lattice planes. According to this XRD analysis for three samples (S1, S3and S32), the sharp peaks with prominent intensity reflect the high crystallinity in these samples of ZnO nanoparticles and the detectable peaks matches well with the JCPDS card (00-036-1451). This may present that the product obtained by solochemical method in this experiment was well crystallized. Studies indicated that the sharp and intense peaks at (101) plane show the growth of ZnO nanoparticles along the easy direction of crystallization of ZnO. Thus, this experimental diffraction pattern confirms that the proposed method of ZnO NPs synthesis, using Zn $(NO_3)_2.6H_2O$ and Zn $(CH_3COO)_2.2H_2O$ as precursors, is suitable for the production of ZnO NPs with sharp peak (Fig, 9). The average crystallite sizes (D) of the ZnO NPs calculated using Debye Scherer formula are about 21.62, 35.97 and 36.16 nm for samples S1, S3 and S32, respectively as tabulated in Tables 1 and 2. In Table 2, the variation in the average crystallite size of samples of ZnO NPs obtained from equal amount of zinc acetate dihydrate (15g) at the same calcination temperature may be due to the variation of exposure times during calcination, environmental influence and the present of some impurities on the surface of the synthesized ZnO NPs.

Generally, the results of ZnO NPs obtained from Zn $(NO_3)_2.6H_2O$) and Zn $(CH_3COO)_2.2H_2O$, as the starting materials, are in a good agreement with previously reported (Marivone, *et al*., 2011; and Mayekar, *et al*., 2014).

Table 3: The XRD parameters and average crystallite sizes of ZnO NPs synthesized using zinc chloride hexahydrate at two different calcination temperatures.

Sample ID &its calcination temperature	Miller Indices (h k l)	2θ (degree)	d-spacing (A)	FWHM=β (A)	Grain Size (nm)	Lattice Parameters(nm)	
						a	c
S2	(100)	31.906	2.80263	0.2039	42.29	0.32	0.56
	(002)	34.577	2.592	0.1852	46.94	0.299	0.52
700^{o}C	(101)	36.406	2.46584	0.1897	49.15	0.285	0.49
	(102)	47.694	1.90528	0.1988	45.61		
2 hrs	(110)	56.746	1.62098	0.2093	45.07		
	(103)	63.015	1.47395	0.2109	46.14		
	(200)	66.522	1.40449	0.2278	43.35		
	(112)	68.094	1.37585	0.214	46.72		
	(201)	69.231	1.35601	0.2148	46.9		
		Average			**45.8**	**0.303**	**0.524**
S4	(100)	31.776	2.81379	0.18	47.93	0.325	0.56
	(002)	34.46	2.60057	0.158	55.11	0.301	0.52
800^{o}C	(101)	36.283	2.47395	0.162	54.02	0.286	0.5
	(102)	47.571	1.90994	0.171	53.08		
2 hrs	(110)	56.61	1.62455	0.183	51.7		
	(103)	62.893	1.47652	0.18	53.87		
	(200)	66.3663	1.40741	0.2346	42.09		
	(112)	67.969	1.37808	0.179	55.78		
	(201)	69.101	1.35823	0.182	56.33		
		Average			**52.21**	**0.304**	**0.526**

The crystalline structure of the samples of ZnO NPs synthesized at 90°C by solochemical reaction between 1.8M NaOH and 0.8M $ZnCl_2.6H_2O$ solution at three different calcination temperatures was also analyzed by XRD technique, as shown in Figure 10 (S2, S22 and S4). The ZnO NPs synthesized from 0.8M $ZnCl_2.6H_2O$ solution was subsequently annealed at different temperatures (600^0C, 700^0C and 800°C) for studying the effect of thermal treatment on the size of ZnO nanoparticles. The diffractogram shows that the products formed exhibit the characteristic diffraction peaks of ZnO with hexagonal wurtzite structure with lattice parameters: a =0.303 nm, c = 0.524 nm at 700℃ (S2) and a = 0.304 nm, c = 0.526 nm at 800℃ (S4) calcination temperature besides the other peaks formed in three samples (Figure 10).These diffraction peaks are probably related to the crystalline planes (100), (002), (101), (102), (110), (200) and (103) of ZnO. However, some diffraction peaks do not match with the diffraction pattern of the ZnO NPs, particularly, those in samples S22 and S2 but with some improvement in sample S4.The average crystallite sizes (D) of samples of ZnO NPs calculated using Debye Scherer formula are about 45.80 and 52.21 nm at calcination temperatures of 700℃ and 800℃ for S2 and S4 sample, respectively. This may indicate the effect of calcination temperatures, high concentration of precursor, the dropping rate, the formation of unwanted compounds such as $Zn(OH)_2$, $ZnCl_2$, $Zn_5(OH)_8Cl_2.H_2O$, the presence of impurity on the surface of ZnO NPs synthesized from $ZnCl_2.6H_2O$, and the incomplete conversion of reactants into the desired ZnO product during the synthesis of ZnO nanoparticles. From this experiment, as the calcination temperature is increased from 700℃ to 800℃, keeping the concentrations of the base and zinc chloride salt precursor constant, the particle size increases atconstant reaction temperature of 90℃. In general, an increased in calcination temperature to 800^0C leads to the increased solubility and hence reduced super saturation of the solution and as a consequence large particles size was obtained. The average particle sizes observed at different calcination temperatures sample of ZnO NPs synthesized from zinc chloride hexahydrate are given in Table 3.

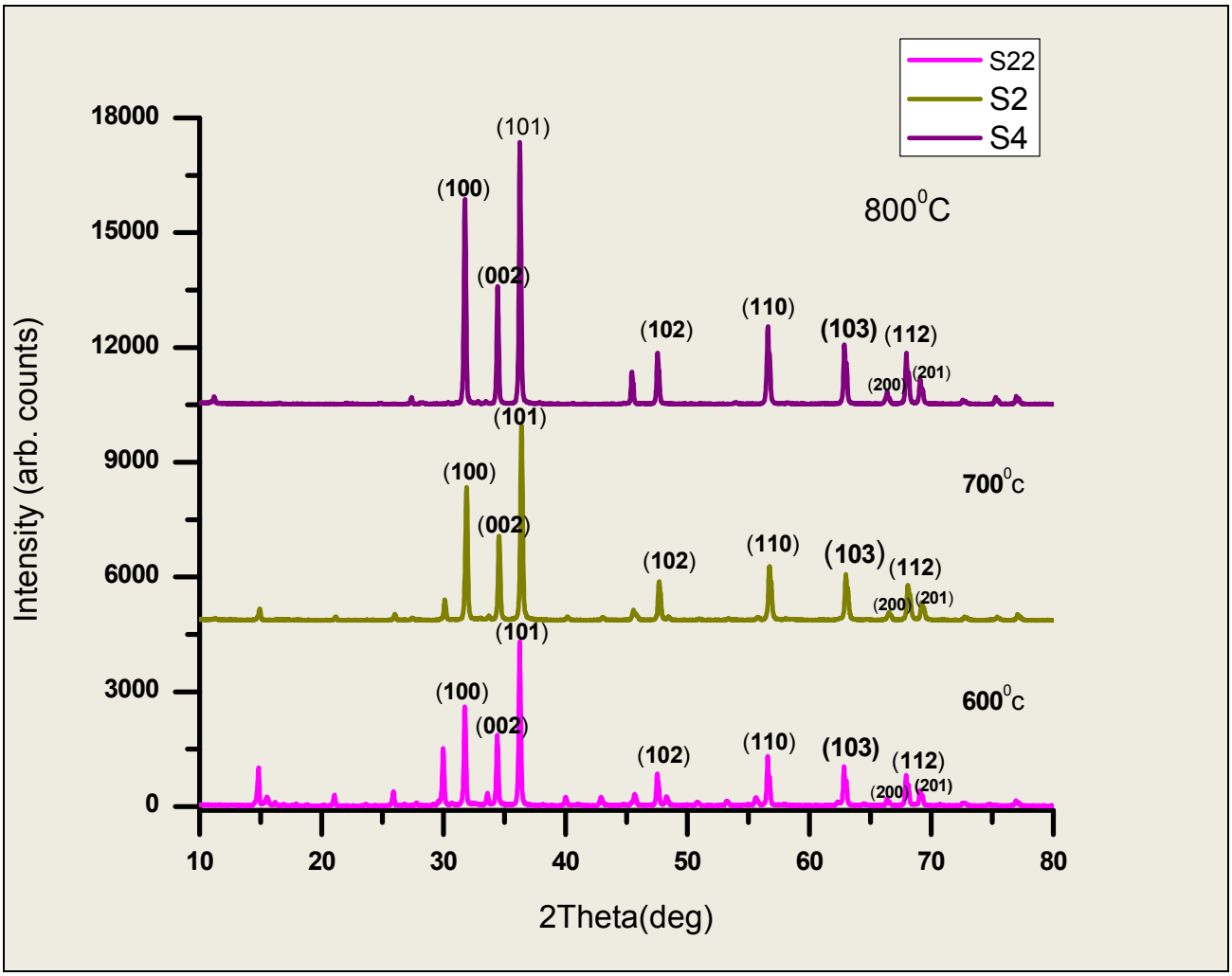

Figure 10:XRD patterns of samples of ZnO NPs synthesized using a 0.8M zinc chloride hexahydrate at three calcination temperatures.

According to previous studies (Parthsarathi and Thilagawathi, 2011 and Rakhshani, 2008), depending on the concentration of the precursor solution, the nanostructures prepared from zinc chloride by chemical or electrochemical methods may exhibit in their composition of ZnO particles mixed with other phases such as $Zn_5(OH)_8 Cl_2.H_2O$ and $Zn(OH)_2$. The presence of these phases in the final composition of the material indicates that the conversion of reactants into the desired ZnO product was not completed especially in S22 and S2 (Fig, 10). Studies indicate that the compound $Zn_5(OH)_8Cl_2.H_2O$ is formed when the concentration of the Zn^{2+}ions is higher than 0.01M (Pradhan and Leung, 2008), which is in agreement with the results obtained in this study,

considering that $Zn_5(OH)_8Cl_2.H_2O$ crystals were produced using 0.8M solution of $ZnCl_2.6H_2O$ as precursor. In addition to this, the literature shows that the $Zn_5(OH)_8Cl_2.H_2O$ can be completely decomposed into ZnO upon calcination at 500 °C or higher. This agrees with the results obtained in this research work by calcinating the powder at 800℃(Figure10 (S4)). This research activity indicates that the formation of the complex compound with ZnO NPs may be also caused by the low reaction temperature (90℃) used in the preparation procedure besides the others parameters such as concentration of the precursor, calcination temperature and time. From previous study, the XRD results indicated that the use of $ZnCl_2.6H_2O$ as precursor alters the composition of the final product, forming ZnO nanocrystals mixed with $Zn_5(OH)_8Cl_2.H_2O$ crystals(Parthsarathi and Thilagawathi, 2011).

Hence, this research activity proves that the XRD results indicate the lower efficiency of the proposed solochemical method in the synthesis of ZnO particles using high concentration of 0.8M$ZnCl_2.6H_2O$ precursor solution at calcination temperature lower than 800℃.In general, from the two spectra of figures 9 and 10, the diffraction peaks obtained are strong and narrow indicating that the nanocrystalline ZnO NPs has good crystallinity. These results may be explained by the nucleation and growth of particles in a solution. Generally, elevation in calcination temperature produces increase in particle size in an ionic liquid due to aggregation and also unevenly sized particles. Increase of crystallinity with increasing calcination temperature was observed by the increase of intensity of the diffraction peaks thereby confirms the statement of previous reports (Hamadanian and Jabbari, 2011).

4.1.3 Fourier transform infrared spectroscopy (FT-IR) analysis

Figure 11 shows the FT-IR spectra of uncalcinated and calcinated samples of ZnO nanoparticles synthesized from zinc nitrate hexahydrate by solochemical method. The FT-IR spectrum of the uncalcinated sample of ZnO NPs (US1) contains a number of peaks from 844 cm^{-1} to 4000 cm^{-1} corresponding to carboxylate (COO-) and hydroxyl (O-H) impurities in the materials (Fig. 11). The broad absorption peaks around 3427-3465 cm^{-1} and 3459 cm^{-1} are assigned to O-H stretching mode of hydroxyl group, which may represent the presence of unwanted excess water molecules on the surface of ZnO nanoparticles, probably due to atmospheric moisture (Fig. 11).

An absorption band has been observed in the uncalcinated sample of ZnO NPs at 2354 cm^{-1} which arises from the absorption of atmospheric CO_2 on the metallic cations (presence of C=O stretching mode).

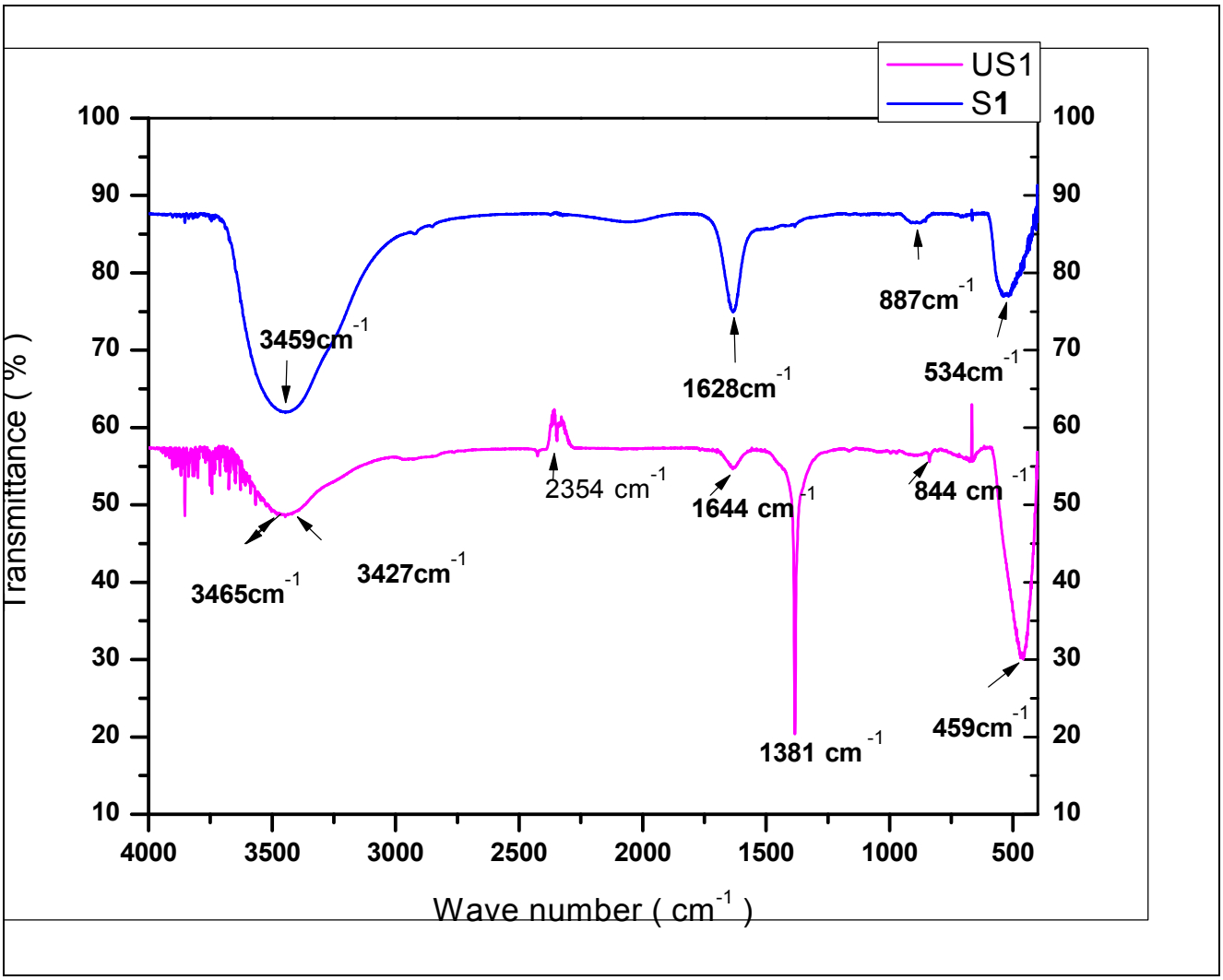

Figure 11: FT-IR Spectra of uncalcinated (US1) and calcinated (S1) sample of zinc oxide NPs synthesized from zinc nitrate hexahydrate precursor.

The strong and sharp peak observed at wave number 459 cm^{-1} clearly showsthe presence of Zn-O stretching mode in the uncalcinated sample of ZnO nanoparticles as shown in Fig.11 (US1). According to the spectrum in Fig.11 (S1), for the pure sample, the intense absorption peak at

wave number (v) = 534 $cm^{-1}$is the characteristic stretching vibrations of metal – oxygen bond formation (Zn-O bond) in the calcinated sample of ZnO NPs. This result indicates the successful production of ZnO nanoparticles by solochemical method. In Figure 11, the bands observed at 1628 and 1644 cm^{-1} are due to asymmetric stretching of carboxylate (or mode of vibration of C=O) which attached to the ZnO nanoparticles during synthesis. The carboxylate probably comes from the reactive carbon containing plasma species during synthesis of ZnO NPs. As the size of nanoparticles increases the contents of carboxylate groups in the sample decrease as shown in Figure 11 (US1 and S1). The peak appearing at 1381 cm^{-1} in the uncalcinated sample of ZnO NPs could be correlated to N=O vibrations and the –COOH bending vibrations of carboxylic acid functional groups are observed at v= 844 cm^{-1}.

Figure 12 (S2 & S4) shows the FT-IR spectra of the calcinated samples of ZnO nanoparticles synthesized from $ZnCl_2.6H_2O$ at 700 ^{0}C and 800 ^{0}C calcination temperature. The broad bands at 3473 and 3451 cm^{-1} correspond to O–H mode of vibration and the asymmetric stretching mode of vibration of C= O was observed between 1626 and 1631 cm^{-1}. The carbon-oxygen-hydrogen bond (C-O-H) bending occurs around 911 $cm^{-1}$and the weak peak at 898 cm^{-1} is due to the C–H bending frequency.

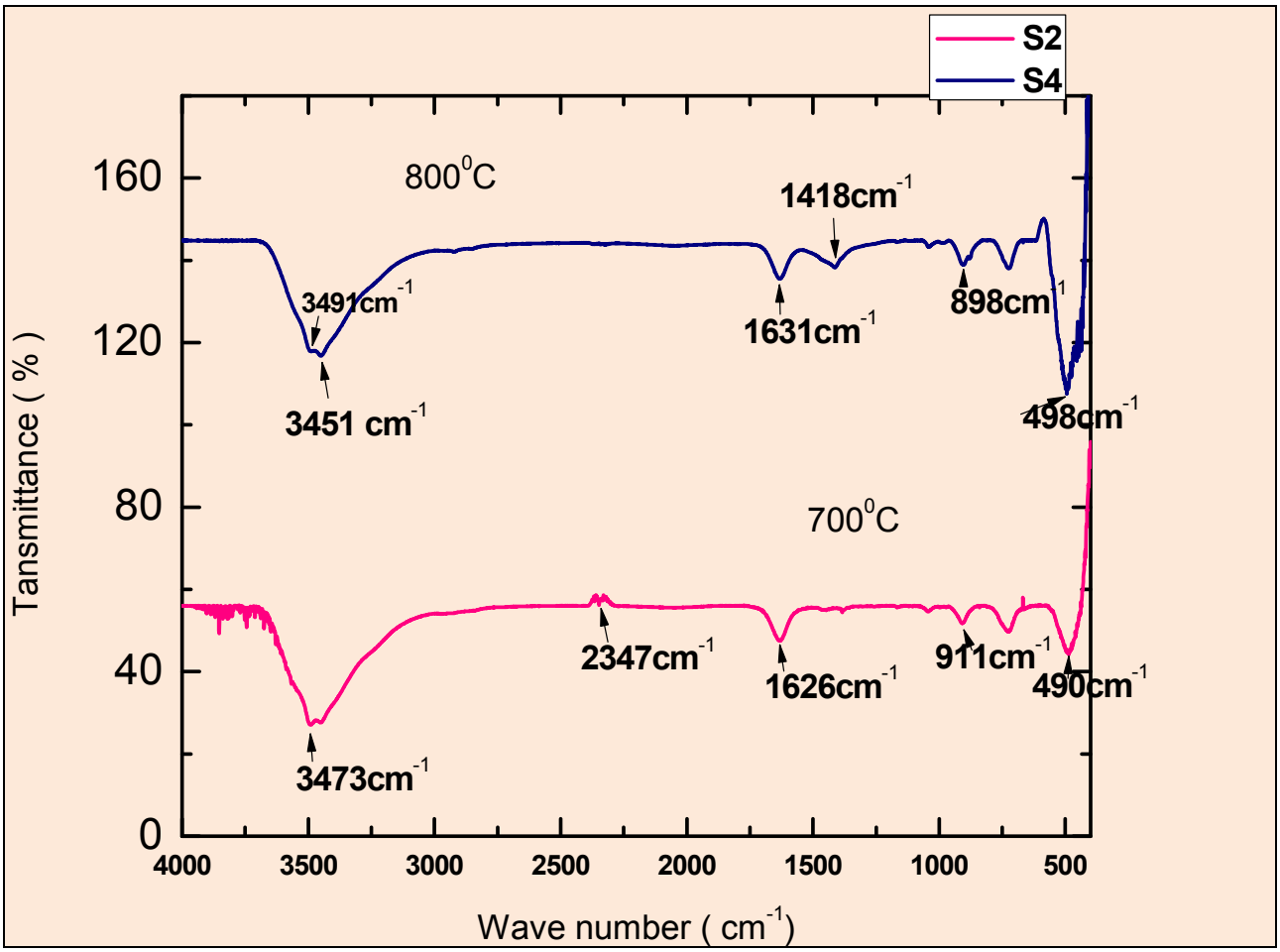

.

Figure 12: FT-IR Spectra of calcinated samples (S2 and S4) of synthesized zinc oxideNPs using zinc chloride hexahydrate precursor at different temperatures.

As the calcination temperature of sample of ZnO nanoparticles increases from 490 to 498 cm^{-1} wave number, the vibration peaks of the bonds in a molecule were shifted up and down which is due to the structural change in the particle size of zinc oxide nanoparticles as observed from the Fig.12 and the symmetric stretching of C=O occurs at v = 1418 cm^{-1}.

Figure 13 shows the infrared absorption spectra of the calcinated sample of ZnO nanoparticles (S3) synthesized from zinc acetate dihydrate in the 4000 - 400 cm^{-1} wave-number ranges. The bands at 3437 cm^{-1} corresponds to the O-H mode of vibration of H_2O, which indicates the existence of water adsorbed on the surface of nanocrystalline powder. The medium asymmetric

mode of vibration of C=O was observed at 1637 cm^{-1}. The weak symmetric stretching occurs around 1394 cm^{-1} because of presence of C-O peak (Fig.13). According to FT-IR spectrum of Fig.13, the absorption peak at 539 cm^{-1} indicates the presence of ZnO nanoparticles synthesized from the hydrated form of zinc acetate at calcination temperature of 400^0C for 12 hrs.

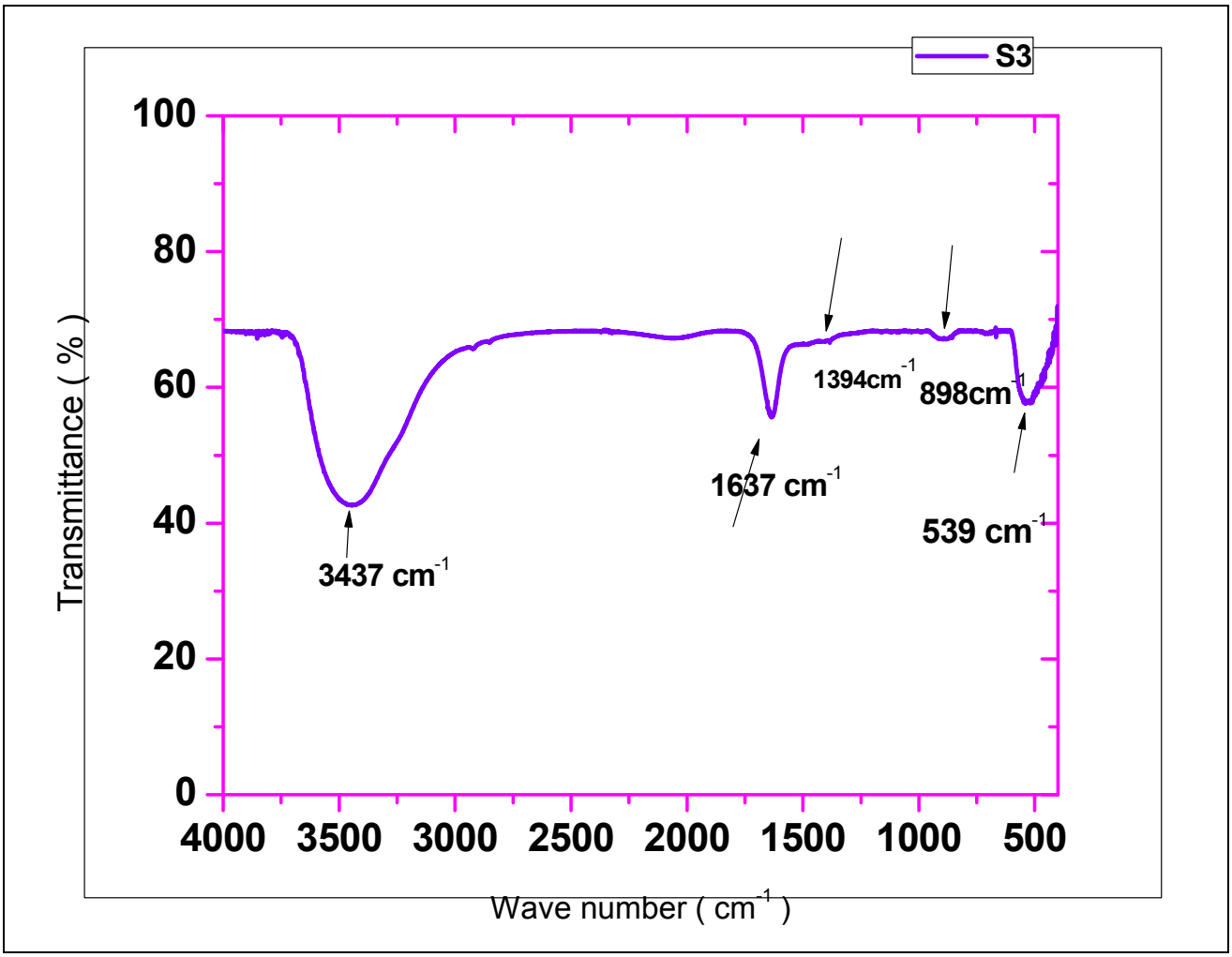

Figure 13: FT-IR Spectra of calcinated sample of synthesized zinc oxide NPs (S3) obtained from zinc acetate dihydrate precursor at 400^0C calcination temperature**.**

In the five spectra of Fig.11, 12 and 13, the Fourier transform infrared spectroscopy (FT-IR) studies showed the absorption peaks at 459, 490, 498, 534 and 539 cm^{-1} for the existence of Zn-O linkage in all samples of ZnO NPs synthesized (Suhandro and Rosari, 2012). This confirms

the formation of zinc oxide nanoparticles in all samples during synthesis process by solochemical method.

4.1.4 Scanning electron microscopy (SEM) analysis

The morphology of ZnO nanoparticles was studied using SEM images. The surface morphology of the synthesized samples of ZnO NPs was viewed through the high resolution scanning electron microscope. SEM images of calcined samples of ZnO NPs, synthesized from zinc nitrate hexahydrate and zinc acetate dihydrate, have different morphologies as shown in Figure 14 (a-g). The morphology of ZnO NPs synthesized from $Zn(CH_3COO)_2.2H_2O$ by solochemical method has agglomerated nanorod shapes (Figure14 (a-d)). On the other hand, the morphology of ZnO nanoparticles synthesized from $Zn(NO_3)_2.6H_2O$ has agglomerated grain types as shown in Figure 14(e-g). From this Figure 14(a-g), the SEM images of the ZnO NPs have different shape and size which are similar with XRD results. The variation of the shape and size of the ZnO NPs is due to the difference in their precursors, sizes of NPs, calcination temperature and time. The SEM images clearly show micro structural homogeneities at high magnification in Figure 14(d&e) and remarkably different morphology for ZnO powder. This indicates that ZnO NPs have successfully prepared using zinc acetate dihydrate and zinc nitrate hexahydrate precursor within a nano range by the solochemical method.

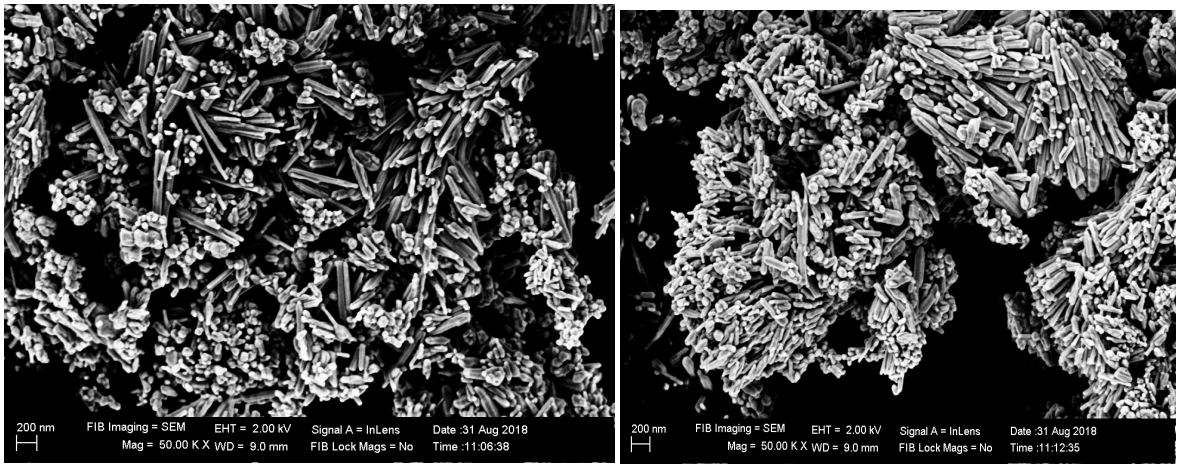

(a) (b)

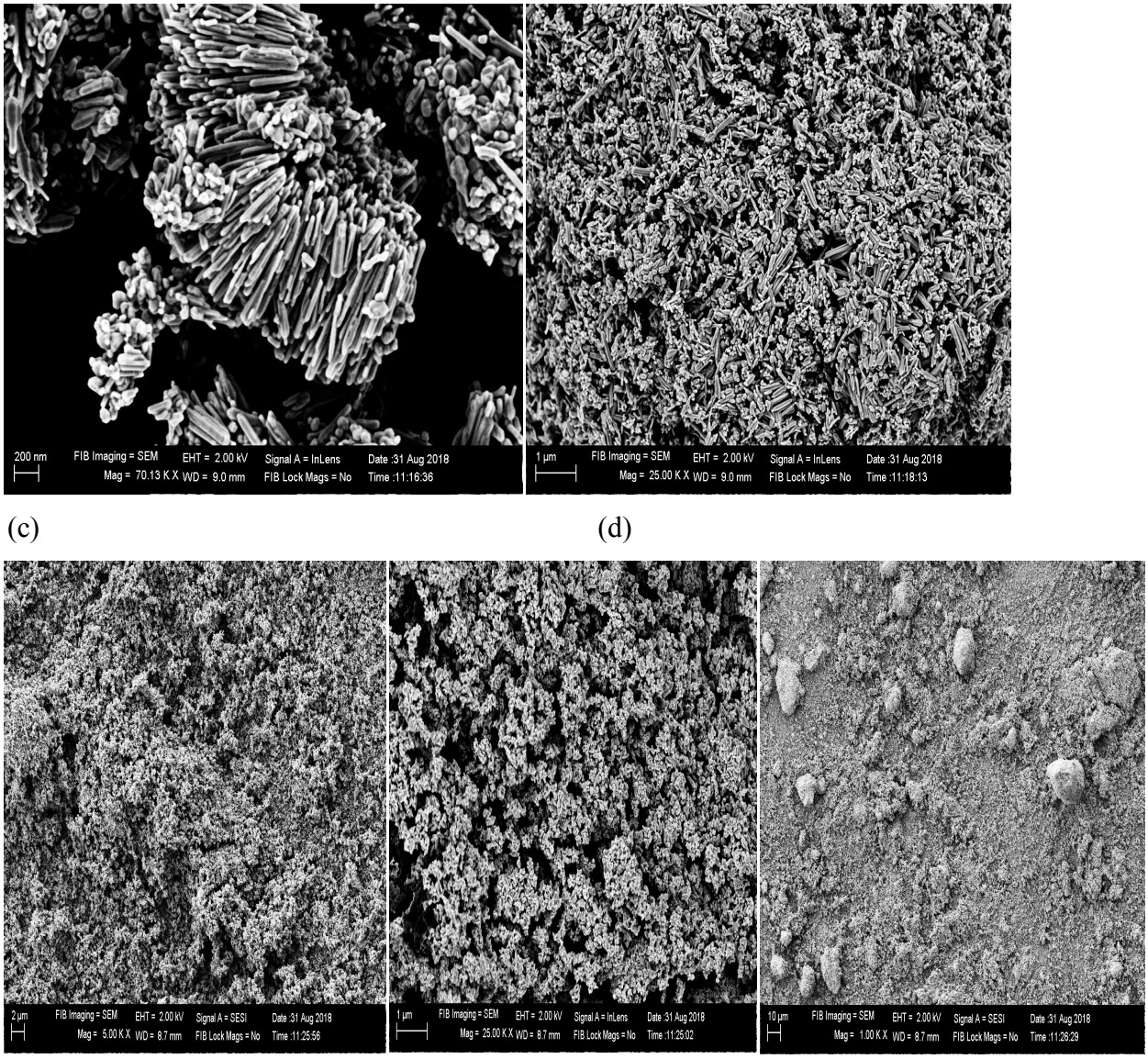

Figure 14: SEM images of ZnO Nanoparticles for samples of S3 (a-d) and S1 (e-g).

4.1.5 Energy dispersive X- ray spectroscopy (EDX)

The Energy Dispersive X-ray Diffractive (EDX) study was carried out for the synthesizedzinc oxide nanoparticles to know about the elemental composition. The energy dispersive X-ray analysis of samples of ZnO nanoparticles synthesized from zinc acetate dihydrate and zinc nitrate hexahydrate at different conditions are shown in Figures 15 to 18.

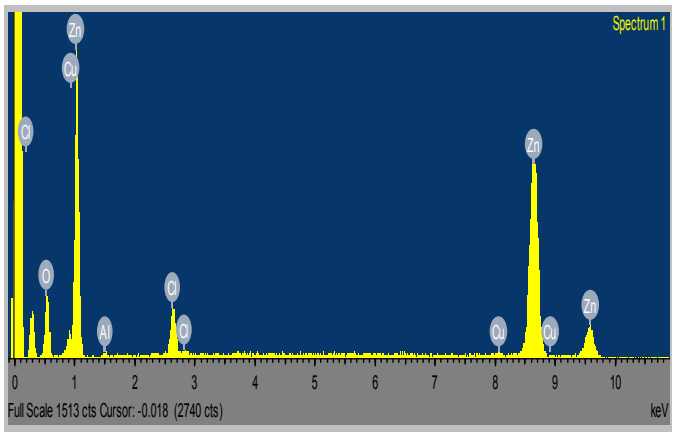

Figure 15: EDX spectrum of S3

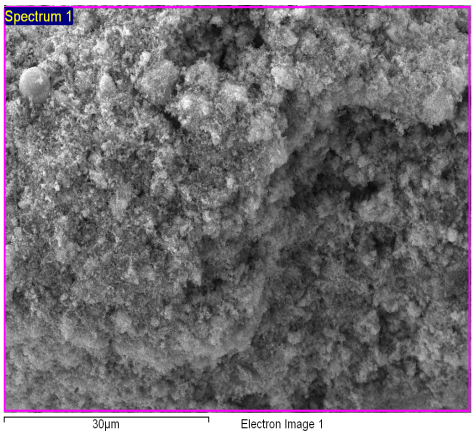

Figure 16: SEM images of selected area for EDX spectra of the sample of S3

Table 4: **Quantitative analysis of sample S3**

Element	Weight%	Atomic%
O k	15.25	39.15
Zn k	81.45	51.18

From the X-ray patterns of Figures (15 &16) and Table 4, this sample contains largely the elements Zn and O in the spectrum (96.7%). This shows that there is very small amount of foreign material present in the spectrum and hence this confirms for the good in the purity of the sample of ZnO NPs synthesized from zinc acetate dihydrate.

The EDX spectrum of Figure 17 with Table 5 shows the sample of ZnO nanoparticles were synthesized using zinc nitrate hexahydrate at reaction temperature of 70^{o}C. EDX confirms thepresence of zinc and oxygen signals of zinc oxide nanoparticle as shown in Figure 17and this analysis showed the peaks that corresponded to the optical absorption of the produced nanoparticle. The elemental analysis of the nanoparticles yielded 84.04% zinc and 11.44% oxygen which prove that the produced nanoparticle is in its highest purified form.

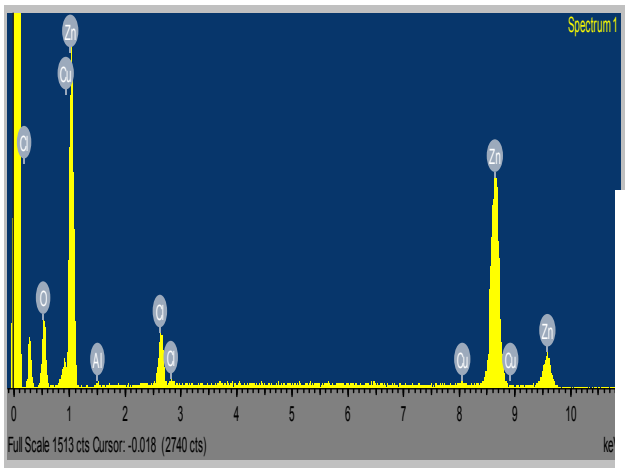

Figure 17: EDX spectrum of S1

Table 5: **Quantitative analysis of sample S1**

Element	Weight %	Atomic %
O k	11.44	33.74
Zn K	84.04	60.66

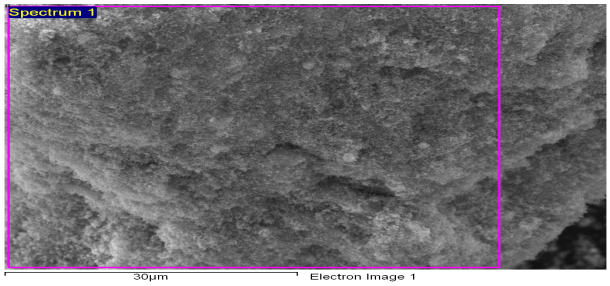

Figure 18: SEM images of selected area for EDX spectra of the sample of S1

4.1.6 The UV-Vis absorbance /reflectance pattern of ZnO nanoparticles

Figure 19(S1, S3) shows the UV-Vis absorbance/reflectance spectra of ZnO nanoparticles synthesized using $Zn(NO_3)_2.6H_2O$ and $Zn(CH_3COO)_2.2H_2O$ at different calcinations temperatures. The absorbance/reflectance peaks of ZnO nanoparticles, synthesized from $Zn(NO_3)_2.6H_2O$ and $Zn(CH_3COO)_2.2H_2O$ precursors, were observed at ranges 323-370 nm at calcinated temperature of 300^{o}C and 400°C, respectively. As temperature increases, the peak absorbance wavelength becomered shifted due to decreasing quantum confinement with increasingparticle size. These peaks are due to electronic transition from deeplevel of valence band to conduction band. The UV-Vis absorbance /reflectance peakvariations among the ZnO NPs are due to the difference intheir size and shape, which results due to the difference in precursors and calcination temperatures (Imran, 2013). Thus at 323nm:

% Absorbance of S3 = 100 - 11.133 = 88.867%

The band gaps energies(Eg) of the samples (S3 and S1)of synthesized ZnO NPs using zinc acetate dihydrate and zinc nitrate hexahydrate were found in the range of 3.84 -3.35 eV. (Figure19).

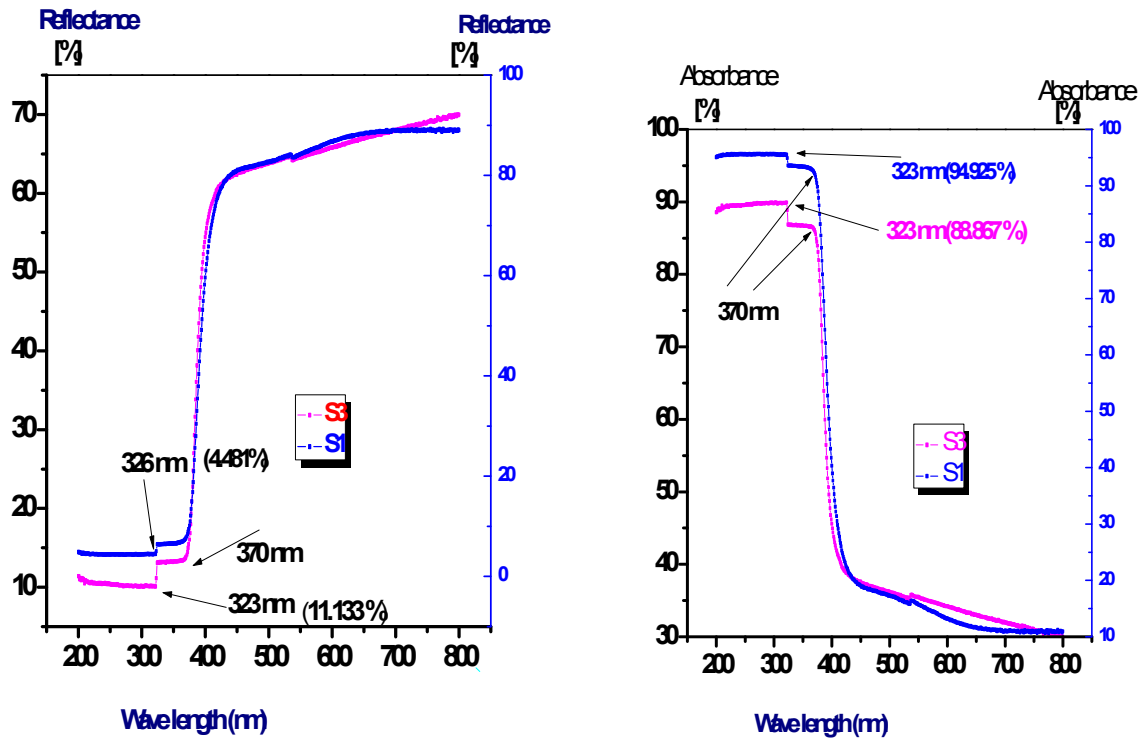

Figure 19: UV-Vis absorbance/reflectance spectra of samples of ZnO nanoparticles synthesized using zinc nitrate hexahydrate (S1) and zinc acetate dihydrate (S3).

4.2 Antibacterial activity of ZnO NPs Synthesized from Three Different precursors

In this work, the antibacterial activity of ZnO NPs synthesized from three precursors was studied against two gram positive (*S. aureus* and *Bacillus subtilis*) and two gram negative (*E. coli* and *Pseudomonas aeruginosa*) bacterial pathogen using agar–well diffusion method through performing tests in nutrient broth and nutrient agar following standard methods. The objectives of using the different precursors in preparing antibacterial agent ZnO NPs by chemical synthesis are of interest to investigate the effects of particle size, shape, temperature, exposure time and concentration on the antibacterial activity of ZnO nanoparticles and to understand the possible mechanisms and activities with four different bacteria. This study was conducted on growth bacteria by loading both uncalcinated and calcinated samples of ZnO NPs synthesized from zinc chloride hexahydrate, zinc nitrate hexahydrate and zinc acetate dihydrate precursors to *S. aureus*,

Bacillus subtilis, Pseudomonas aeruginosa and *E. coli* with three different concentrations of samples of ZnO NPs prepared (C1= 10, C2= 20 and C3= 30 mg/ml) on each bacterium to study the growth behavior of bacteria and determine the antibacterial activity of ZnO NPs. The comparative antibacterial activity of ZnO nanoparticles synthesized from these precursors against those selected bacteriais shown in the Figure 20 (a – e). The activity was determined by noting the zones of inhibition around the wells. The clear zones of inhibition around the wellswere the evidence of antibacterial activity of ZnO nanoparticles, which are presented in Figure 20 (a – d).

(a) **S. *aureus*** (b) **P. *aeruginosa*** *(c)* **S. *aureus*** **(d) E. *coli***

(e)

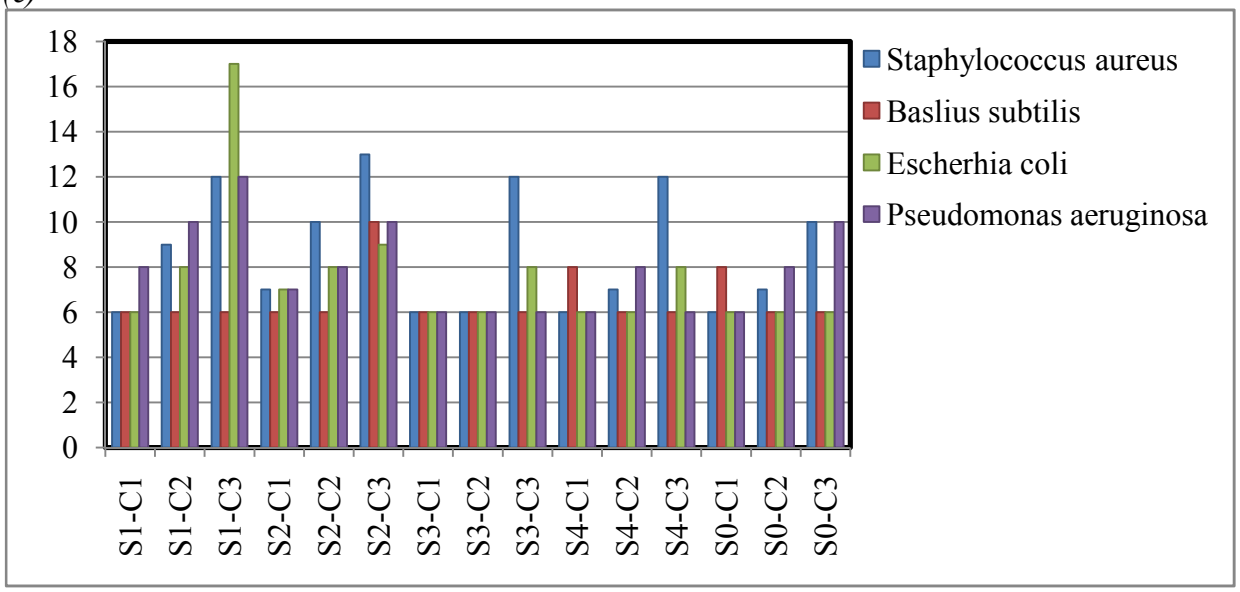

Figure 20: The comparison of antibacterial activity of some calcinated/uncalcinated samples of ZnO NPs synthesized on selected bacteria andanti bacteria assessment by parallel streak method.

When assessed for antibacterial activity by agar well diffusion method, the ZnO nanoparticles synthesized from uncalcinated zinc nitrate hexahydrate (US1=S0), calcinated zinc nitrate hexahydrate (S1) and Zinc chloride hexahydrate (S2) showed a maximum inhibitory effect against *Pseudomonas aeruginosa, E. coli* and *S. aureus* with zone of inhibition diameters of 12, 17 and 13 mm, respectively, and are shown in the Figure 20 and summarized in Table 6. Among those concentrations, ZnO NPs at a concentration of 30 mg/ml sample shows high toxicity and inhibitory effect against the growth of S. *aureus***,** *P. aeruginosa* and E. *coli* bacteria, as shown in Table 6 and Figure 20. This mayexplain the antibacterial activity of nanoparticles is increased as the concentration of ZnO NPs is increased by reducing the growth of microorganism (Fig.20 and Table 6).

Table 6: Zone of inhibition diameters (in mm) of samples of ZnO NPs synthesized from the three different precursors against gram positive and gram negative bacterial strains.

Strain group	Gentamycin 30μg	Inhibition Zone Diameter (in mm)														
		Sample ID														
		S1			S2			S3			S4			US1= S0		
		C1	C2	C3	C1	C2	C3	C1	C2	C3	C1	C2	C3	C1	C2	C3
S. aureus	17	6	9	12	7	10	13	6	6	12	6	7	10	8	9	10
B. subtilis	12	6	6	6	6	6	10	6	6	6	8	6	6	6	6	6
E. coli	15	6	8	17	7	8	9	6	6	8	6	6	6	9	8	6
P. *aeruginosa*	14	8	10	12	7	8	10	6	6	6	6	8	10	6	10	12

From Table 6 and Fig 20, ZnO NPs synthesized from the three zinc salts' precursors are sensitive to a gram positive bacterium (*S. aureus*) and two gram negative bacteria (*E. coli* and *P. aeruginosa*) but they are almost more resistant to *Basilius subtilis*. These results illustrate that ZnO NPs has good antibacterial activity against *S. aurous*, *E. coli* and *P. aeruginosa* for all samples. The reason for this may be due to the antibacterial action resulted in this study is to be dependent on the activity of ZnO and method employed. Besides method, antimicrobial susceptibility testing results can also be affected by many other factors, such as the microorganisms tested and the degree of solubility of ZnO NPs in dimethyl sulfoxide. Some researchers reported that the damage of the bacterial cell membrane and extrusion of the cytoplasmic contents may be due to ZnO which causing in the death of the bacterium (Dobrucka and Długaszewska, 2015). Other researchers have also indicated the disruption of bacterial membranes may be triggered by the production of ROS (Ashe, 2011). Among the bacterial classes tested, only the gram-positive Basilius subtilis was found to be particularly resistant to the ZnO NPs synthesized by this method. The reason behind this fact may be gram-positive

bacterium of Basilius subtilis has tough cell wall and the size of nanoparticles does not match with the thickness of cell wall because of the low concentration of nanoparticles.

The good antibacterial activities to three different microorganisms of the samples with the synthesized ZnO (calcinated or uncalcinated) may be due to the binding to the oxide NPs of ZnO, the crystallinity of ZnO NPs, the size and the concentration of sample, and the surface area- to- volume ratio of ZnO. The unique characteristics of NPs largely increases the surface area of ZnO or enhance the affinity, so the calcinated sample of ZnO NPs (S1) exhibits stronger antibacterial activity than uncalcinated sample of ZnO NPs (US1) as shown in the Table 6 and Fig 20. According to the results in Table 6, it can be concluded that the antibacterial activity of ZnO nanoparticles increased with decreasing particle size and increasing powder concentration of ZnO nanoparticles. In general, this study revealed that the ZnO NPs synthesized from the hydrated forms of Zinc nitrate, Zinc chloride and Zinc acetate have budding antibacterial activity against *S. aureus*, *E. coli* and *P. aeruginosa* bacteria.

5. Conclusions and Recommendations

5.1 Conclusions

ZnO nanoparticles were synthesized using various routes from different precursors. The solochemical method proved a successful synthetic route in terms of its cost, ease of handling, rapidity, versatility, simplicity, and environmental friendliness. Moreover, it is confirmed that thevarious applications of ZnO nanoparticles depend upon the control of both physical andchemical properties such as size, size dispersity, shape, surface reactivity, crystal structure,organization onto a support, and dispensability. In addition, these factors mainly dependupon the synthetic method. Therefore, shape, size, and dispersity can be controlled bytuning different parameters during the synthesis process, e.g., the precursor type, concentration, types of solvent, reaction time, reaction and calcination temperature.The XRD study confirms the formation of hexagonal wurtzite structure of the synthesized ZnO nanoparticles with the average crystallite sizes of 21.62,35.97, 36.16 and 45.8 nm. This shows, the use of different salt precursors, calcination temperatures and times leads to change in the particle sizes of nanoparticles. The vibrational phonon of ZnO observed in the range of 459 - 539 cm^{-1} confirms the successful production of ZnO NPs.SEM images reveal that the particles appearto be almost nanoroad and grain in shape. The synthesized ZnO NPs were also applied for antibacterial applications using agar well diffusion method. All the three ZnO NPs have been shown admirable antibacterial activity compared to the standard antibiotic drugs on *S. aureus*, *E. coli* and *P*. a*eruginos*a bacteria. However, at 30 mg/ml, the ZnO NP synthesized using a $Zn(NO_3)_2.6H_2O$ precursor was revealed excellent antibacterial activity than the two precursors against S. aureus and E. coli. Generally, this study revealed that the ZnO NPs synthesized from the hydrated forms of Zinc nitrate, Zinc chloride and Zinc acetate have potential antibacterial activity against gram-positive (*S. aureus)* and gram- negative (*E.coli* and *P*. a*eruginos*a*)* bacteria.

5.2Recommendations

Regarding future aspect of ZnO nanoparticles, one can conclude that although there are various reports regarding ZnO nanoparticles synthesis with various shapes and sizes, there is stilla lack of quality synthesis in terms of crystallinity, size, and sphericity of the particles and the non-use of organic solvents, which may hinder its possible application in biomedical sciences (or in evaluation its antibacterial activity). Application of ZnO nanoparticles in the biological realm requires high qualityZnO nanoparticles in aqueous solution at neutral pH and physiological temperature,because biomolecules are very sensitive to changes in temperature and pH. During the synthesis of ZnO nanoparticles from zinc chloride hexahydrate, chloride ion testing and then washing the sample several times after calcination should be needed in order to remove the impurities from the products.

Please add recommendation

What you like to advice for the improvement of the quality synthesis in terms of crystallinity, size, and sphericity

6. REFERENCES

Abd El-Latif M.M. and El-kadyM.F.(**2011**).Synthesis, characterization and evaluation of Nano zirconium vanadiate ion exchanger by using three different techniques. *Material Researchbulletin.,*46, 105-118.

Amna S., Shahrom M., Azman, Noor H. M., LingK. , SitiC. A., HabsahK. M.,Dasmawati M .(**2015**). Review on Zinc Oxide Nanoparticles: Antibacterial Activity and Toxicity Mechanism. *Nano-Micro Lett*. , 7, 219–242.

Aromal S. A., VidhuVK., Philip D .(**2012**).Green synthesis of well dispersed gold nanoparticles using Macrotyloma uniform. *SpectrochimActa Part A.,* 85, 99–104.

Ashe B. A.(**2011**).Detail investigation to observe the effect of zinc oxide and Silver nanoparticles in biological system [dissertation]. *Department of Biotechnology & Medical Engineering, National Institute of Technology,Rourkela, India* , 10,2.

CaoH.L., QianX.F., GongQ., DuW. M., MaX. D.,and ZhuZ. K.(**2006**).Nanotechnology,17, 3632.

Cha S.H., Hong J., Mcguffie M., Yeom B., Vanepps J.S., KotovN.A. (**2015**).Shape-Dependent Biomimetic Inhibition of Enzyme by Nanoparticles and Their Antibacterial Activity.*ACS Nano*, 9, 9097–9105.

ChenC.(**2007**). Investigation of nano - sized ZnO Nanoparticles. *Mater.Lett.,* 61, 2961 – 2964.

CullityB. D. and StockS. R**.(2001**).Elementary of X-ray Diffraction, third ed., Englewood Cliffs.

Daraio C.,Jin S.,Silva G.A. and Parpura V.**(2012**).Synthesis and Patterning Methods for NanostructuresUseful for Biological Applications.*Nanotechnology for Biology and Medicine, ed.,54,* 27–44.

DemianetsL. N., KostomarovD. V., KuzminaI. P. and PushkoS. V.(**2002**).*Crystallogr. Rep.*, 47, 586.

Dobrucka R. and DługaszewskaJ.(**2015**). Biosynthesis and antibacterial activity of ZnO nanoparticles using Trifolium pretense flower extract. *Saudi Journal of Biological Sciences.*

Duan J-X, Wang H and Huang X-T.(**2007**). Synthesis and characterization of ZnO ellipsoid-like nanostructures.*Chinese Journal of Chemical Physics,* 20, 613-618.

El-Kemary M., H. El-Shamy and I. El-Mehasseb, (**2010**). Photocatalytic degradation ofciprofloxacin drug in water using ZnO nanoparticles.*J. lumin.*130, 2327–2331.

FuG., VaryP.S., LinC.T. (**2005**). TiO_2nanocomposites for antimicrobial coatings. *J. Phys. Chem.* B, 109, 8889–8898.

Gericke M., Pinches A.(**2006**).Biological synthesis of metal nanoparticles. *Hydrometallurgy*, 83, 132–140.

Hamadanian M.andJabbariV. (**2011**). Higher-education Institute, Mashhad, Iran, 21, 12-14.

Hu Y. and Chen H.J. (**2008**), Preparation and characterization of nanocrystalline ZnO particles from a hydrothermal process, J. *Nanopart. Res*., 10, 401-407.

Imran K. (**2013**). Structural and optical properties of Zr doped ZnO nanoparticles. *Optmater*, 35,1189-1193.

JonesN., RayB., RanjitK. T., and MannaA. C. (**2008**). " Antibacterial activity of ZnO nanoparticle suspensions on a broad spectrum of microorganisms," *FEMS MicrobiolLe*tt., 279, 71-76.

Jung W., Koo H., Kim K., Shin S., Kim S. and Park Y. (**2008**).Antibacterial activity and mechanism of action of the silver ion in Staphylococcus aureus and Escherichia coli.*Applied and Environmental Microbiology*, 74, 2171-2178.

Kaushik N., Thakkar MS., Snehit S., Mhatre MS., Rasesh Y., Parikh MS .(**2010**).Biological synthesis of metallic nanoparticles.*Nano med Nanotechnology BiolMed* ,6, 257–262.

KoserJ. (**2011**) .“Synthesis of ZnO nanoparticle using different concentration of capping agent,” *International Journal of Technology Innovations and Research*, 16, 1–7.

Koudelka l., Horak J., Jariabk P.(**2004**).Morphology of polycrystalline ZnO and its physical properties.*Journal Materials Science*, 29, 1497-1500.

KWON Y., KIM H., LIM C., SHIM K.(**2002**).Characterization of ZnO nano powders synthesized by the polymerized complex method via an organ chemical route.*Journal of Ceramic Processing Research*, 3, 146-149.

LiM., ZhuL., LinD. (**2011**). Toxicity of ZnO nanoparticles to Escherichia coli: mechanism and the influence of medium components. *Environ. Sci. Technol*., 45, 1977–1983.

Li Y., Zhang W., Niu J., Chen Y. (**2012**).Mechanism of Photo generated Reactive Oxygen Species and Correlation with the Antibacterial Properties of Engineered Metal-Oxide Nanoparticles. *ACS Nano*, 6, 5164–5173.

Liu X .and Yu W. (**2006**). "Evaluating the Thermal Stability of High Performance Fibers by TGA". *Journal of Applied Polymer Science*.99: 937–944.

Look D.C., Reynolds D.C., Jones R.L., Litton C.W., Cantwell G., Eason D.B. (**2002**).Characterization of homo epitaxial p-type ZnO grown by molecular beam epitaxy. *Applied Physics Letters*, 81,1830-183

Makhluf S., DrorR., Nitzan Y., Abramovich Y., Jelinek R. and GedankenA. (**2005**). Microwave-assisted synthesis of nanocrystallineMgO and its use as a bacteriocide.*Advanced Functional Materials*, 15,1708-1715.

Manna A. C.(**2012**).Synthesis, Characterization, and Antimicrobial Activity of Zinc Oxide Nanoparticles. *Nano-Antimicro- bails: Progress and Prospects, Berlin: Springer Press,34,* 151-180.

Marivone,JeaneG.,AR.,Gilvan,SB.,Carlos,EMC.,Humberto .(**201**1).Synthesis of ZnO nanostructures in low reaction temperature. Florianópolis, SC, Brasil.

Mayekar J., Dhar V., RadhaS. (**2014**) Role of salt precursor in the synthesis of zinc oxide nanoparticles. *International Journal of Research in Engineering.*

Meisam H., Mahmood A., Hamid H. (**2016**).In-situ study of mass and current density for electro phoretic deposition of zinc oxide nanoparticles‖.*Ceramics International, Elsevier*, 6, 6906-6913.

Morris J. (**2011)**. How safe is our food? *Journal of Emerging Infectious Diseases*, 17, 126-128.

OzgurU., HofstetterD.,MorkoH. (**2010**). ZnO Devices and Applications: *A Review of Current Status and Future Prospects‖, Proceedings of the IEEE,*7, 1255 - 1268.

Parthsarathi V. and ThilagawathiG.(**2011**).Synthesis and characterization of zinc oxide nanoparticle and its application on fabrics for microbe resistant defence clothing. *International Journal of Pharmaceutical Sciences*, 3, 392-398.

PengX., PalmaS., FisherN.S., WongS.S.(**2011**).Effect of morphology of ZnO nanostructures on their toxicity to marine algae; *Aquat. Toxicol*. , 3, 186–196.

Perez-Lopes O.W., Faria A.C., Marcilio N.R., Bueno J.M.C.(**2005**). The catalytic behavior of zinc oxide prepared from various precursors and by different methods. *Materials Research Bulletin*.

Pradhan D and Leung KT. (**2008**).Controlled growth of two-dimensional and one-dimensional ZnO nanostructures on indium tin oxide coated glass by direct electro deposition. *Langmuir,*24, 9707-9716.

Prellier W., Foucheta A., MerceyB.(**2003**).Oxide-diluted magnetic semiconductors: A review of the experimental status. *Journal of Physics Condensed Matter*, 15, 1583.

Raghupati, Koodali, R. T.and Manna, A. C. (**2011**).Size-dependent bacterial growth inhibition and mechanism of antibacterial activity of zinc oxide nanoparticles.*Langmuir*, 27, 4020-4028.

RahmanP. (**2009**). Green, Nanoscale, 1, 214–224.

Rajneesh, K .S.,Sheo, K .M., Prakash, S .G .(**2012**). ZnO nanoparticles: Structural, optical and photoconductivity characteristics. *Journal of Alloys and Compounds*, 539, 1-6.

Rakhshani, A.E.(**2008**). Boron-doped ZnO films grown by successive chemical solution deposition.*Journal of Physics D: Applied Physics* , 41, 1-6.

Rao,C.N.R.,A.M llerandCheethamA.K.(**2004**).The Chemistry of Nanomaterials: Synthesis, Properties and Applications,1, 741.

RezendeC.P., da SilvaJ.B., MohallemN.D.(**2009**). *Brazilian Journal of Physics*, 1, 248

Robert F., AgisA., Iliadis and Peter K.(**2003**). *Journal of Applied Polymer Science*,1, 1058.

Sawai J.(**2003**). Quantitative evaluation of antibacterial activities of metallic oxide powders (ZnO, MgO and CaO) by conductimetric assay. *Journal ofMicrobiological Methods* , 54, 177 - 182.

SobhaK., Surendranath K. and MeenaV.(**2010**).Biotechnology and Molecular Biology Reviews, 5,01.

SrinivasaRaoN.(**2015**).Structural and optical investigation of ZnO nano powders synthesized from zinc chloride and zinc nitrate. *American Journal of Materials Science, 5*, 66 - 68.

Stuart B. (**2004**). Infrared Spectroscopy Fundamentals and Applications.

SuhandroP.andRosariS.(**2012**).Synthesis and spectroscopic characterization of undopednanocrystalline ZnO nanoparticles prepared by co-precipitation.*Journal of Material Science and Applications,* 3, 530-537.

Sundrarajan M., Suresh J. and Gandhi R. (**2012**). A comparative study on antibacterial properties of MgO nanoparticles prepared under different calcination temperature.*Digest Journal of Nanomaterials and Bio structures*, 7, 983-989.

TongX., DuF., LiangY., HuQ., WuN., GuanG., HuX.(**2013**). Polymorphous ZnOcomplex architectures: selective synthesis, mechanism, surface area and Zn-polar plane-code- termining antibacterial activity: *J. Mater. Chem. B*.,1, 454–463.

VidyasagarC C. ,ArthobaNaikY., VenkateshaT G. and ViswanathaR.(**2012**). *Nano-Micro Lett*.4 , 73.

ViswanathaR., AmenitschH., and SarmakineticsD.(**2007**). *Am. Chem. Soc*., 129, 4470.

WahabR., KimY., MishraA., YunS., ShinH. (**2010**).Formation of ZnO micro-flowers prepared via solution process and their antibacterial activity. *Nanoscale Res. Lett*., 5, 1675– 1681.

WenJ., ZhuK., LiY.,andSongJ. (**2014**).“High temperature mixing hydrothermal synthesis of ZnO nanocrystal with wide growth window,” *Current Applied Physics*, 14, 359– 365.

Yoshio W., E.M., Kozo S. (**2011)** .X - Ray Diffraction Crystallography Introduction, Examples and Solved Problems.

Zanni E., Chandraiahgari C.R., Bellis G.D., Montereali M.R., Armiento G., Ballirano P., Polimeni A., Sarto M.S., UccellettiD. (**2016**). Zinc Oxide Nano roads-Decorated Grapheneanoplatelets and A Promising Antimicrobial Agent against the Cariogenic Bacterium Streptococcus mutans. *Nanomaterials*, 6, 179.

ZhangJ.(2011). Silver-coated zinc oxide nano antibacterial synthesis and antibacterial activity characterization. *International Conference on Electronics and Optoelectronics (ICEOE)*, 3, 94–98.

ZhangJ., SunL. D., L. D. YinL. D., SuH. L., LiaoC. S., and YanC. H.(**2002**). *Chem. Mater*., 14, 4172.

Zhang L., DingY., Povey M., York D.(**2008**).ZnO nano-fluids -A potential antibacterial agent. *Progress Nat Sci*. , 18, 939-944.

ZhangL., JiangY., DingY., PoveyM., YorkD.(**2007**).Investigation into the antibacterial behaviour of suspensions of ZnO nanoparticles (ZnO nanofluids).*J.Nanopart. Res*.,9, 479–489.

ZhangX., YanS., TyagiR. D. andSurampalliR. Y.(**2011**). Chemosphere, 82, 489–494.

ZhangY., RamM.K., StefanakosE.K., GoswamiD.Y.(**2012**).Synthesis, characterization, and applications of ZnO nanowires.*J. Nanomater*, 12, 1–22.

7. APPENDICES

Appendix 1:XRD pattern for calcinated sample of ZnO NPs synthesized from zinc nitrate hexahydrate (S1).

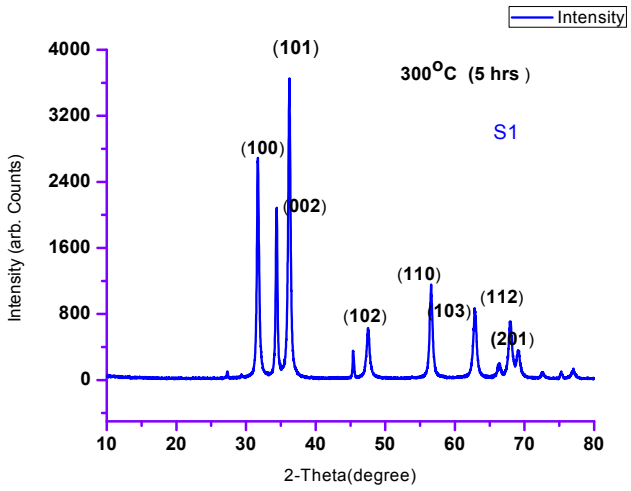

Appendix 2: XRD pattern for calcinated sample of ZnO NPs synthesized from zinc acetate dihydrate (S3) at 400°C calcination temperature for 12 hrs.

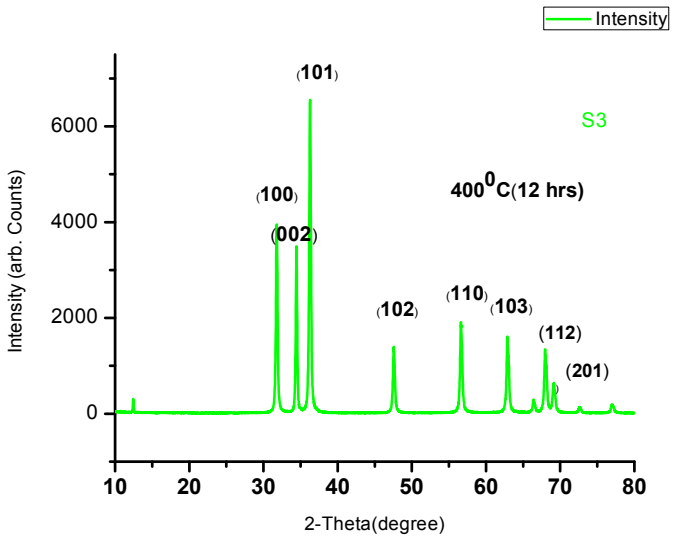

Appendix 3: XRD pattern for calcinated sample of ZnO NPs synthesized from zinc acetate dihydrate (S32) at 400°C calcination temperature for 2 ½ hrs**.**

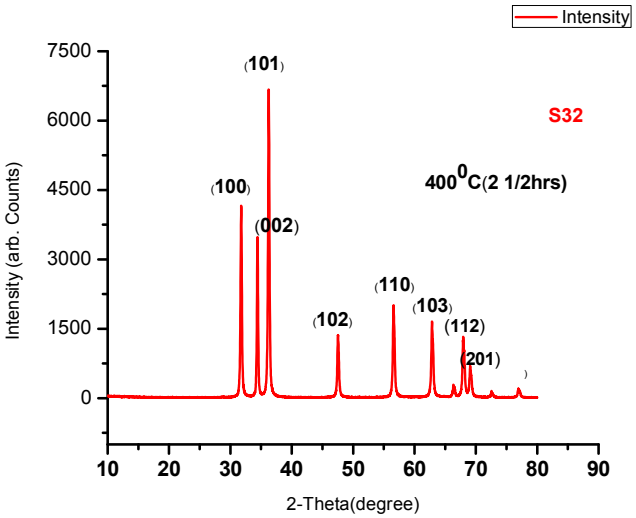

Appendix 4: XRD pattern for calcinated sample of ZnO NPs synthesized from zinc chloride hexahydrate (S**2**) at 700^{o}C calcination temperature for 2 hrs

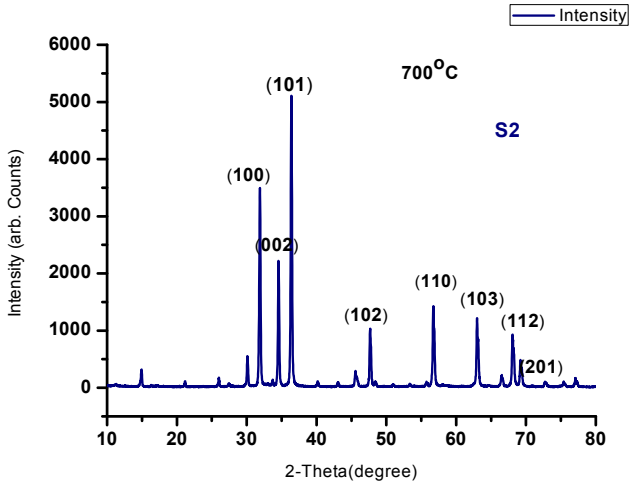

Appendix 5: XRD pattern for calcinated sample of ZnO NPs synthesized from zinc chloride hexahydrate (S4) at 800^{o}C calcination temperature for 2 hrs.